ACS Catalysis

Subscriber access provided by READING UNIV

Article

Mechanistic Insights on Pd/Cu-Catalyzed Dehydrogenative Coupling of Dimethyl Phthalate

Masafumi Hirano, Kosuke Sano, Yuki Kanazawa, Nobuyuki Komine, Zen Maeno, Takato Mitsudome, and Hikaru Takaya

ACS Catal., **Just Accepted Manuscript** • DOI: 10.1021/acscatal.8b01095 • Publication Date (Web): 15 May 2018

Downloaded from http://pubs.acs.org on May 15, 2018

Just Accepted

"Just Accepted" manuscripts have been peer-reviewed and accepted for publication. They are posted online prior to technical editing, formatting for publication and author proofing. The American Chemical Society provides "Just Accepted" as a service to the research community to expedite the dissemination of scientific material as soon as possible after acceptance. "Just Accepted" manuscripts appear in full in PDF format accompanied by an HTML abstract. "Just Accepted" manuscripts have been fully peer reviewed, but should not be considered the official version of record. They are citable by the Digital Object Identifier (DOI®). "Just Accepted" is an optional service offered to authors. Therefore, the "Just Accepted" Web site may not include all articles that will be published in the journal. After a manuscript is technically edited and formatted, it will be removed from the "Just Accepted" Web site and published as an ASAP article. Note that technical editing may introduce minor changes to the manuscript text and/or graphics which could affect content, and all legal disclaimers and ethical guidelines that apply to the journal pertain. ACS cannot be held responsible for errors or consequences arising from the use of information contained in these "Just Accepted" manuscripts.

ACS Publications

is published by the American Chemical Society. 1155 Sixteenth Street N.W., Washington, DC 20036

Published by American Chemical Society. Copyright © American Chemical Society. However, no copyright claim is made to original U.S. Government works, or works produced by employees of any Commonwealth realm Crown government in the course of their duties.

Mechanistic Insights on Pd/Cu-Catalyzed Dehydrogenative Coupling of Dimethyl Phthalate

Masafumi Hirano,*,† Kosuke Sano,† Yuki Kanazawa,† Nobuyuki Komine,†Zen Maeno,‡, § Takato Mitsudome,*,‡ and Hikaru Takaya*,¶

†Department of Applied Chemistry, Graduate School of Engineering, Tokyo University of Agriculture and Technology, 2-24-16 Nakacho, Koganei, Tokyo 184-8588, Japan

‡Department of Materials Engineering Science, Graduate School of Engineering Science, Osaka University, 1-3 Machikaneyama, Toyonaka, Osaka 560-8531, Japan

¶Institute of Chemical Research, Kyoto University, Gokashou, Uji, Kyoto 611-0011, Japan

Supporting Information

ABSTRACT: Despite industrial importance, very limited mechanistic information on the dehydrogenative coupling of dimethyl phthalate had been reported. Herein we report the detailed mechanism for dehydrogenative coupling of dimethyl phthalate catalyzed by $[Pd(OAc)_2]$/$[Cu(OAc)_2{\cdot}H_2O]$/1,10-phenanthroline·H_2O (phen·H_2O). The solution-phase analysis of the catalytic system by XANES shows the active species to be Pd(II) and the EXAFS supports the formation of an (acetato)(dimethyl phthalyl)(phen)palladium(II) complex from $[Pd(OAc)_2]$. A formation pathway of tetramethyl 3,3',4,4'-biphenyltetracarboxylate via disproportionation of independently prepared $[Pd(OAc)\{C_6H_3(CO_2Me)_2\text{-}3,4\}(phen)]$ is observed with regeneration of $[Pd(OAc)_2(phen)]$.

KYEWORDS: *dehydrogenative coupling, dimethyl phthalate, mechanism, Pd-catalysis, XAFS*

INTRODUCTION

Transition-metal mediated formations of biaryls are powerful and indispensable approaches to produce electronic materials, liquid crystals, and pharmaceutical molecules. The synthetic methods of biaryls involve the Ullmann coupling, the cross-coupling, and the direct arylation. They are reliable but they need to prepare a halogenated compound and/or arylmetal compound in advance. The other problem is emission of wastes from the reaction. The dehydrogenative coupling of arenes is the most straightforward coupling between arenes, which is generally catalyzed by a Pd complex with a Cu co-catalyst in the presence of oxygen. This is a halogen-free process and one can directly use aromatic compounds as reactants with high atom economy. However, efficiency of the catalysis is still limited.

The first catalytic dehydrogenative coupling was reported by Itatani and Yoshimoto for the coupling of toluene catalyzed by $[Pd(OAc)_2]$ (**1a**).[1] They also reported dehydrogenative coupling of dimethyl phthalate (**3**) to give tetramethyl 3,3',4,4'-biphenyltetracarboxylate (**4**) along with small amounts of the regioisomer, tetramethyl 2,3,3',4'-biphenyltetracarboxylate (**5**), catalyzed by **1a**/$[Cu(OAc)_2{\cdot}H_2O]$ (**2a**·H_2O)/1,10-phenanthroline·H_2O (phen·H_2O) (eq. 1).[2] Such a Wacker-type catalyst system works only under sufficiently diluted conditions, and this reaction requires harsh conditions. The total product yield is mostly less than 10%. Nevertheless, this process is operated in an industrial plant for production of monomers for polyimides.

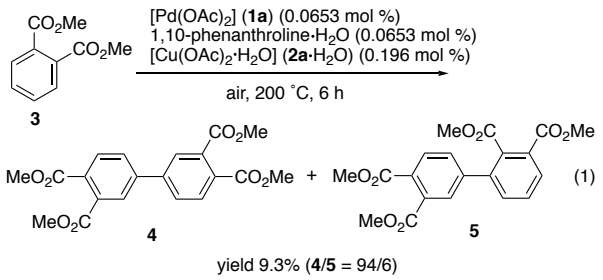

According to the analogy of the Wacker-type catalysis, the dehydrogenative arene coupling is generally proposed to proceed as shown in Scheme 1. Namely, [Pd(OAc)$_2$L] gives [Pd(OAc)ArL] probably by the internal electrophilic substitution (IES)[3-7] or electrophilic aromatic substitution mechanism (step A). The resulting [Pd(OAc)ArL] reacts with second arene, as observed by Hartwig[8] and Ozawa[9] to give [PdAr$_2$L] (step B), or [PdAr$_2$L] is produced by disproportionation reaction of [Pd(OAc)ArL] (step C) as suggested by the detailed kinetic study using *o*-xylene by Stahl and co-workers.[10] Then, the reductive elimination from [PdAr$_2$L] occurs to give the biaryl product and [PdL], which is oxidized by 2 equiv of [Cu(OAc)$_2$L] to regenerate [Pd(OAc)$_2$L] (step E).

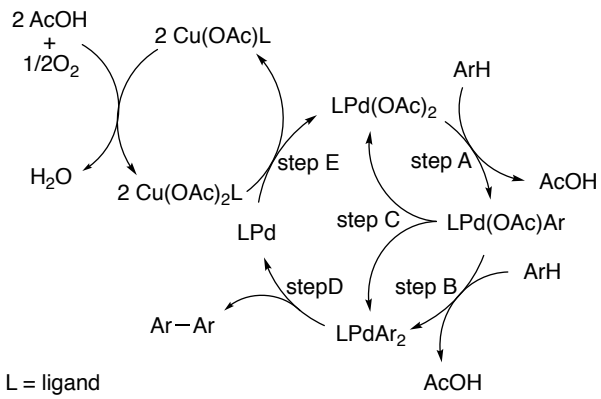

Scheme 1. Putative Mechanism for Dehydrogenative Arene Coupling.

Since such dehydrogenative arene coupling of **3** is operated under harsh conditions in the presence of paramagnetic copper species, observation of the catalyst system by conventional NMR experiments and isolation of the key intermediate is difficult. The detailed mechanism has therefore been largely unknown.

In this paper, we report the mechanistic insight on the dehydrogenative coupling of **3** by the solution-phase XAFS (X-ray absorption fine structure) using a synchrotron radiation. To our best knowledge, Stluts, Friedman and co-workers were the first to bring the synchrotron XAFS in a study of homogeneous catalysts using a Rh complex.[11] Following the pioneering study, homogeneous catalysts involving Ti,[12] V,[13] Cr,[14] Mo,[15] Mn,[16] Fe,[17] Ru,[18] Ni,[19] Pd,[20] Au[21] and Cu[22] were studied by XAFS. Note that one of the authors succeeded to elucidate the mechanism of paramagnetic Fe-catalyzed Kumada-Tamao-Corriu coupling by the solution-phase XAFS analysis.[17c] The reviews for XAFS analysis of homogenous catalysts have been reported.[23] Nevertheless, detailed mechanistic study of homogenous catalysis using XAFS remains difficult. The problems include inherently poor signal-to-noise ratio, a result of low concentration of catalyst and background absorption by organic materials.[23b] In other words, a well-considered approach is indispensable to gain distinct evidences from the XAFS experiments. In order to shed light on the ambiguous mechanism for Pd/Cu-catalyzed dehydrogenative arene coupling of **3**, we prepared putative intermediates according to the working hypothesis shown in Scheme 1 by alternative methods. With their single crystal X-ray structure analysis, NMR studies, and their stoichiometric and catalytic reactions, we obtained a solid evidence on the mechanism by the XAFS studies.

RESULTS AND DISCUSSION

Synthesis of Putative Intermediates. [Pd(OAc)$_2$(phen)] (**1b**) was prepared from [Pd(OAc)$_2$] (**1a**) according to literature method (Scheme 2).[24] Because Sakaki and co-workers have shown the C–H bond cleavage of benzene by [Pd(O$_2$CR)$_2$] to give [Pd(O$_2$CR)Ph] in the Fujiwara-Moritani reaction,[4a] the putative intermediates in this process are [Pd(OAc){C$_6$H$_3$(CO$_2$Me)$_2$-3,4}(phen)] (**1c**) and [Pd(OAc){C$_6$H$_3$(CO$_2$Me)$_2$-2,3}(phen)] (**1d**). According to the modification of the literature method,[25] complex **1c** was newly prepared by the oxidative addition of dimethyl 4-bromophthalate to [Pd(dba)$_2$] in the presence of tmda followed by the treatments with phen·H$_2$O and AgOAc (route A in Scheme 2). On the other hand, the oxidative addition of dimethyl 3-bromophthalate to [Pd(dba)$_2$] was almost ineffective (less than 3% yield). However, the oxidative addition of dimethyl 3-iodophthalate to [Pd(dba)$_2$] in the presence of phen·H$_2$O gave [PdI{C$_6$H$_3$(CO$_2$Me)$_2$-2,3}(phen)] (**1e**) in 78% yield, which eventually gave **1d** by the treatment with AgOAc in 91% yield (route B). These new complexes were fully characterized by ^{1}H and ^{13}C NMR and elemental analysis, and **1c** was also characterized by X-ray structure analysis (Figure 1). The X-ray structure of **1c** is consistent with the structure estimated by NMR. The Pd(1)–N(1) distance [2.123(3) Å] is significantly longer than Pd(1)–N(2) [2.034(3) Å], which suggests strong trans influence of C(4) in the dimethyl phthalyl group. The selected bond distances for **1c** are listed in Table 1, along with the related Pd complexes.

In the ^{1}H NMR spectrum of **1c** in dmso-d_6, the all resonances assignable to the phen ligand were observed inequivalently because of the different ligands in the trans positions in a square planar geometry. Upon warming to 80 °C, the inequivalent phen resonances eventually coalesced to be equivalent.

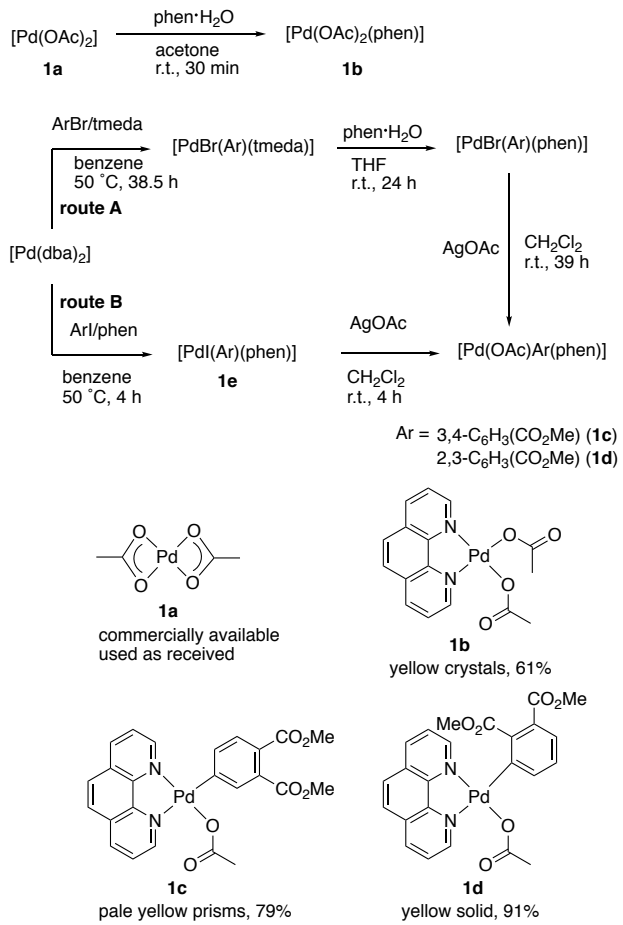

Scheme 2. Preparations of [Pd(OAc)$_2$(phen)] (1b), [Pd(OAc){C$_6$H$_3$(CO$_2$Me)$_2$-3,4}(phen)] (1c) and [Pd(OAc){C$_6$H$_3$(CO$_2$Me)$_2$-2,3}(phen)] (1d).

This phenomenon can be explained either by (*i*) reversible dissociation of the phen ligand, (*ii*) rapid and reversible reductive elimination between the acetato and 3,4-dimethyl phthalyl groups,[27] (*iii*) reversible dissociation of the acetato ligand, or (*iv*) twist-rotation via pseudotetrahedral transition state.[28] We conducted the

Table 1. Selected Bond Distances of Pd Complexes 1b, 1c and 1e (Å).

	1b[a]	1c	1e
Pd(1)–N(1)	2.002(3)	2.123(3)	2.127(3)
Pd(1)–N(2)	2.018(3)	2.034(3)	2.072(3)
Pd(1)–C(4)	---	1.984(4)	---
Pd(1)–O(5)	---	2.023(3)	---
Pd(1)–C(1)	---	---	1.992(3)
Pd(1)–O(1)	2.017(3)	---	---
Pd(1)–O(3)	1.999(3)	---	---

[a]The bond distances of **1b** was taken from ref. 26.

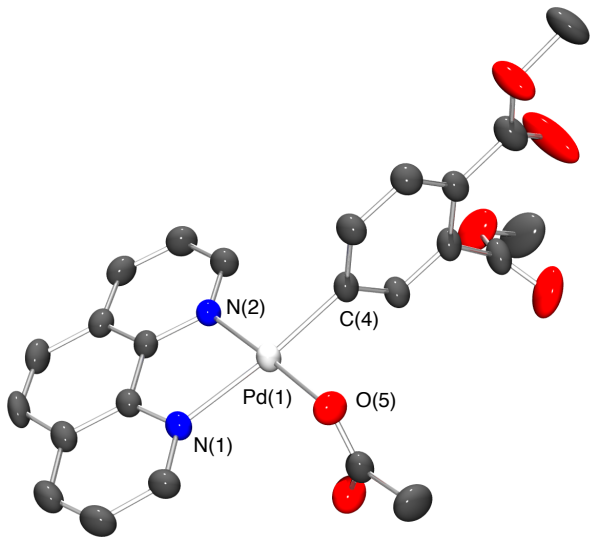

Figure 1. Molecular structure of [Pd(OAc){C$_6$H$_3$(CO$_2$Me)$_2$-3,4}(phen)] (1c) by X-ray with selected numbering schemes. All hydrogen atoms are omitted for clarity. Ellipsoids represent 50% probability.

variable temperature NMR experiments of **1c** in the presence of added phen ligand.

Although the added free phen resonances broadened at high temperature, almost no effect on the dynamic behavior of **1c** was observed (*cf.* SI). Figure 2 shows the variable temperature ^{1}H NMR spectra for **1c** (left) and **1d** (right) in the presence of added NaOAc. A significant broadening of the acetate resonances of **1c** and NaOAc was observed even at 30 °C and they were reversibly coalesced around 70 °C. This behavior clearly shows exchange of the acetato ligand in **1c** with NaOAc (mechanism iii) on the NMR time-scale, and a reversible dissociation of the acetato ligand in **1c** is suggested in dmso-d_6 (eq 2). A dmso-d_6 molecule presumably coordinates to the cationic Pd(II) species and both *O*- and *S*-bound dmso complexes of cationic Pd(II) are reported.[29] The added phen is presumably perturbed by some interaction with resulting coordinatively unsaturated species.

In relation to this fact, Itami, Studer and co-workers proposed a similar dissociation of the acetato ligand from

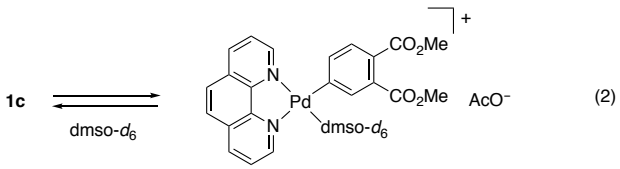

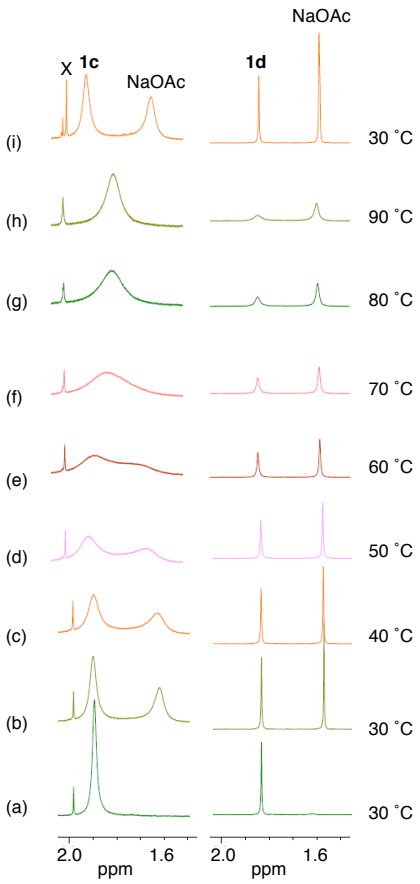

Figure 2. Variable temperature ^{1}H NMR spectra of [Pd(OAc){$C_6H_3(CO_2Me)_2$-3,4}(phen)] (1c) (left) and [Pd(OAc){$C_6H_3(CO_2Me)_2$-2,3}(phen)] (1d) (right) in the region of the acetato groups (400 MHz, dmso-d_6). (a): before addition of NaOAc, (b)-(i): after addition of 1 equiv of NaOAc. × indicates an impurity.

[Pd(Ar)(OAc)(bpy)] in the C4-selective arylation of thiophenes.[30] Yu and co-workers also suggested dissociation of the acetato ligand from [PdX(OAc)(phen)].[31] The present observation may also support these proposals.

In the case of **1d**, although broadening of the acetato ligand and added NaOAc resonances were observed in the range 50-90 ˚C in ^{1}H NMR (Figure 2, right), no trend of coalescence was observed. Note that no broadening of the added phen resonances was observed for **1d**. Probably, **1d** also releases the acetato group at high temperature but the event is much slower than **1c**.

Attempts to make single crystals of **1d** failed but we obtained single crystals of the precursor [PdI{$C_6H_3(CO_2Me)_2$-2,3}(phen)] (**1e**) suitable for X-ray structure analysis. The molecular structure of **1e** by X-ray is depicted in Figure 3.

We also performed the DFT calculations to obtain the optimized structures of **1c** and **1d**. Figure 4 shows the top

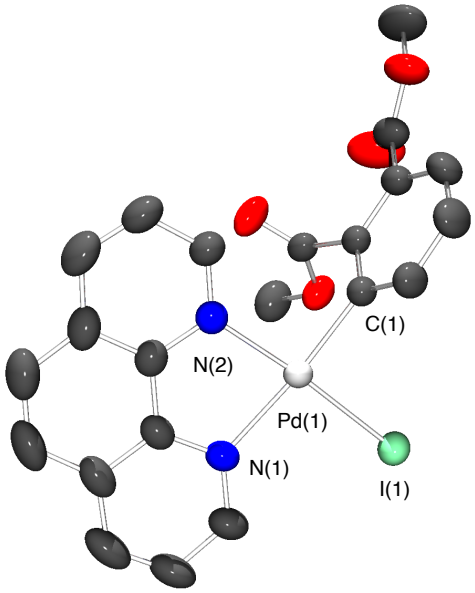

Figure 3. Molecular structure of [PdI{$C_6H_3(CO_2Me)_2$-2,3}(phen)] (1e) by X-ray with selected numbering schemes. All hydrogen atoms are omitted for clarity. Ellipsoids represent 50% probability.

and side views of a merged structures of **1c** and **1d**. Interestingly, these optimized structures show high coincidence among the acetato, phen and the *ipso* carbons in the dimethylphthalyl groups. Their major differences can be found in the deviation of the planes between the square plane constituted by the Pd center and the benzene-ring in dimethylphthalyl group [118.7˚ (**1c**) and 81.1˚ (**1d**)]. We will discuss about these optimized structures in the section of XAFS studies.

Other Compounds. Preparation of [Pd(OAc)$_2$(phen)] (**1b**) from commercially available **1a** was well-established,[24,32] and the molecular structure of **1b** by X-ray analysis was also reported.[26] We made single crystals of **1b** for this study according to literature method.[26] We also prepared [Cu(OAc)$_2$(phen)] (**2b**).[33] Although the molecular structure of **2b** by X-ray has been already reported,[34] we independently solved the molecular structure of **2b**.

The target product **4** was obtained by the dehydrogenative coupling of dimethyl phthalate (**3**) and the molecular structure of **4** was unequivocally determined by X-ray structure analysis (Figure 5). This molecule has the 2-fold axis in the molecule, suggesting a very symmetric structure and the C–C bond length between the aryl groups is 1.491(3) Å. The dihedral angle between two biaryl planes are –0.2(3)˚, suggesting to be a planar molecule.

Stoichiometric Reactions of Dimethylphthalylpalladium(II) Complexes. Because preparation and isolation of **1c** from **1a** or **1b** was difficult, the reverse

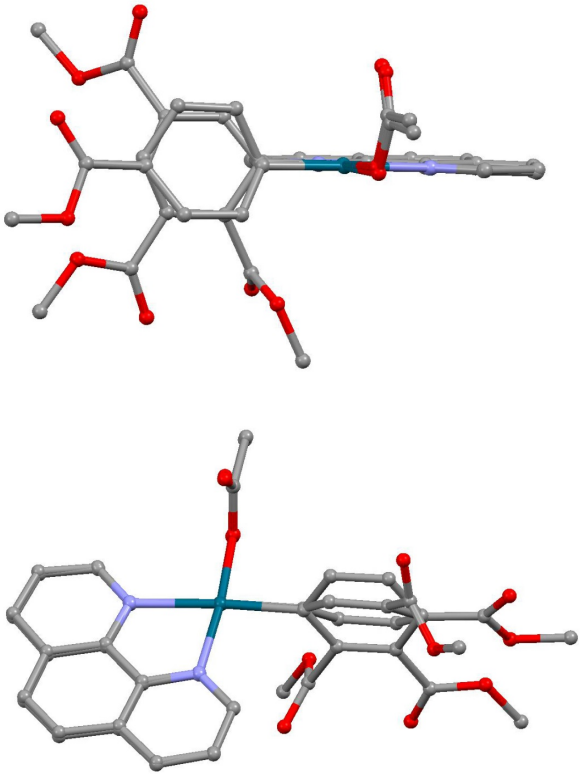

Figure 4. Top and side views of a merged structure of 1c and 1d optimized by the DFT calculations.

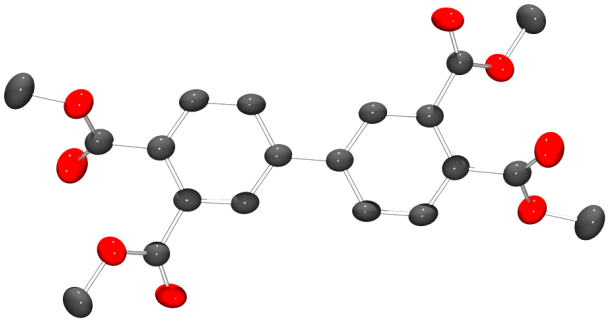

Figure 5. Molecular structure of tetramethyl 3,3'4,4'-biphenyltetracarboxylate (4). All hydrogen atoms are omitted for clarity. Ellipsoids represent 50% probability.

reaction, formation of **1b** from **1c**, was conducted. Treatment of **1c** with acetic acid at 100 ˚C for 30 min produced **1b** and dimethyl phthalate (**3**) in 98% and 78% yields, respectively (eq. 3).

A similar treatment of **1d** with acetic acid also produced **1b** (96%) and **3** (87%). According to the view of microscopic reversibility, these backward reactions make the connection between **1b** and **1c** or **1d**. A related study concerning microscopic reversibility between $[Hg(O_2CR)_2]$ and $[Hg(O_2CR)Ph]$ has been documented.[35]

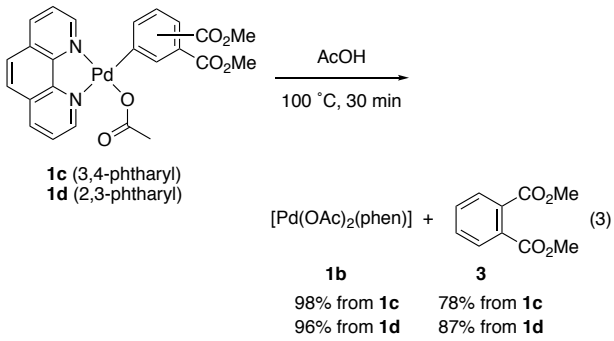

Pyrolysis of **1c** at 180 ˚C resulted in the formation of **4** in 60% (30%/Pd) yield, suggesting disproportionation reaction of **1c** under these conditions (eq 4). When **1d** was treated under the same conditions, however, no coupling product was observed at all and small amount of dimethyl phthalate (**3**) was observed in 10% yield. Pyrolysis in the presence of both **1c** and **1d** produced a mixture of **4** (21%) and **5** (4%), and **6** was not observed at all (eq 5). Dimethyl phthalate (**3**) was also not observed in this reaction. These results suggest one of the possible pathways to give **4** and **5** to be a disproportionation reaction of **1c**, and transmetallation between **1c** with **1d**. In addition, the present result also suggests that disproportionation reaction of **1d** does not occur.

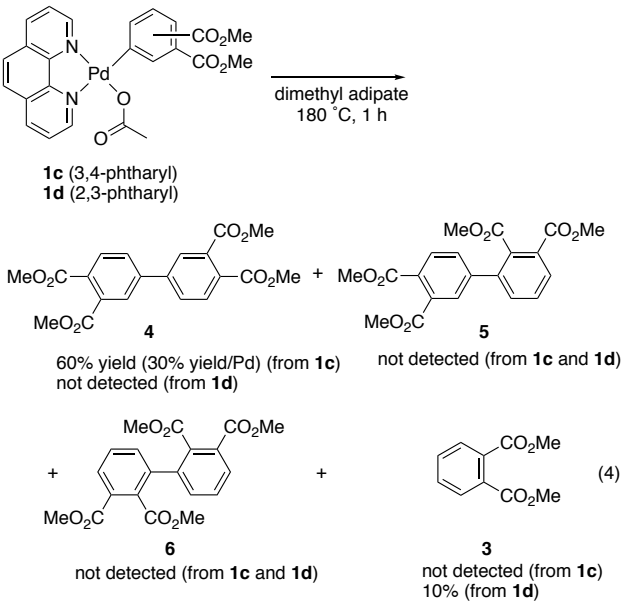

As discussed above, the variable temperature NMR suggests that **1c** reversibly dissociates the acetato anion at elevated temperature. Osakada and co-workers documented the disproportionation reaction of PdIArL (L = tmeda, bpy, Me_2bpy) to proceed from a cationic $[PdArL_2]^+$ complex giving a biaryl.[36] They noted strong

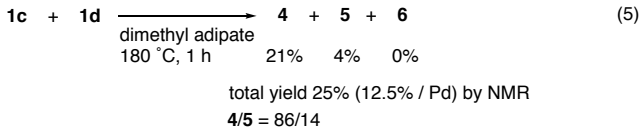

dependence of the reaction on the solvent used, and acetone was the best solvent for disproportionation reaction. When we conducted the reaction of [PdBr{$C_6H_3(CO_2Me)_2$-3,4}(phen)] with $AgBF_4$ in acetone, however, no biaryl product was observed. After screening of the solvents, we found the reaction in dimethyl phthalate (**3**) produced **4** in 62% yield (eq 6). The reaction also produced **4** in CH_2Cl_2, although the yield was not particularly high (21%). Note that neither of the regioisomers **5** nor **6** were observed in these reactions. These reactions, and pyrolysis of **1c**, suggest formation of **4** by the disproportionation reaction/reductive elimination at Pd(II) species.

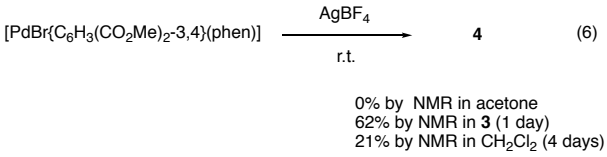

In order to generate a putative [Pd{$C_6H_3(CO_2Me)_2$-3,4}$_2$(phen)], reactions of [PdX{$C_6H_3(CO_2Me)_2$-3,4}(phen)] (X = Br, OAc) with dimethyl 4-(pinacolboryl)phthalate were conducted. According to a similar reaction reported by Osakada and co-workers,[37] Ag_2O would promote this transmetallation. However, present reactions were very sluggish even in the presence of Ag_2O, and complex mixtures involving **4** were obtained (**4**: 43-53 % yield) (Scheme 3). The transmetallation product [Pd{$C_6H_3(CO_2Me)_2$-3,4}$_2$(phen)] was not observed during the reactions. A similar treatment of [Pd(OAc){$C_6H_3(CO_2Me)_2$-3,4}(phen)] (**1c**) with diethyl 4-(pinacolboryl)phthalate gave **7** in 42% yield along with trace amount of **4** (2%). These experiments suggest the *in situ* formation of diarylpalladium(II) species by the transmetallation to release **4** or **7** by the reductive elimination. By taking into account all these stoichiometric reactions, the present formation of **4** is consistent with the disproportionation reaction of **1c** followed by reductive elimination from a bis(3,4-dimethyl phthalyl)palladium(II) species. Osakada and co-workers proposed disproportionation of cationic $[PdAr(solvent)(bpy)]^+$ via a dinuclear dicationic Pd species $[(bpy)ArPd(\mu^2\text{-}Ar)Pd(bpy)(solvent)]^{2+}$,[36] and such dinuclear dicationic species may also play a key role in the present reaction.

Catalytic Dehydrogenative Coupling of Dimethyl Phthalate. Catalytic dehydrogenative couplings of dimethyl phthalate (**3**) were screened under the conditions of Pd catalyst (4.00 mM), 1,10-phenanthroline·H_2O (4.00 mM), Cu co-catalyst (1.20 mM) in **3** (25 mL) under air

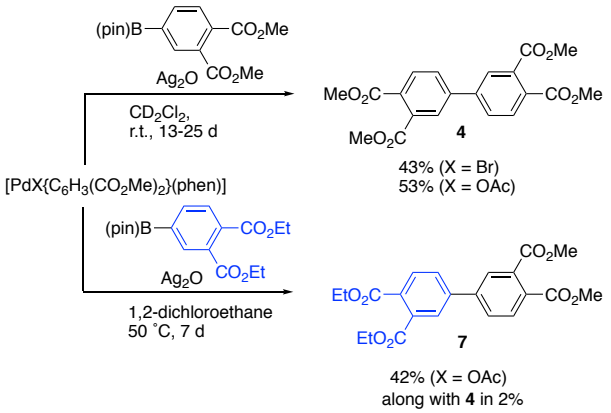

Scheme 3. Transmetallations of PdX{$C_6H_3(CO_2Me)_2$-3,4}(phen)] (X = Br, OAc) with dialkyl 4-(pinacolboryl)phthalate.

(0.1 MPa) at 200 ˚C for 6 h as the standard set of conditions (Table 2). The catalyst system involving [Pd(OAc)$_2$] (**1a**: 0.065 mol %)/[Cu(OAc)$_2$·H_2O] (**2a**·H_2O: 0.020 mol %)/[phen·H_2O] (0.065 mol %) produced the biaryls in 8.5% yield (**4**/**5** = 90/10) with 64 TONs (entry 1), which was almost consistent with the reported catalysis (eq. 1).[2] The reaction was completely shut-down in the absence of phen (entry 3). Without use of copper co-catalyst, the product yield was significantly diminished (entry 4). [Cu(OAc)$_2$(phen)·0.5H_2O] (**2b**·0.5H_2O), [Cu(acac)$_2$] (**2c**) and [Cu(OAc)] (**2d**) were found to be promising co-catalysts (entries 4-6). Although Mitsudome, Kaneda and co-workers documented the Cu-free Wacker reaction of electron-deficient internal alkenes,[38] the present reaction did not work well in the absence of a Cu complex (entry 7). [Pd(OAc)$_2$(phen)] (**1b**) also showed similar catalytic properties (entries 8-13).

When [Pd(OAc){$C_6H_3(CO_2Me)_2$-3,4}(phen)] (**1c**) was used as the catalyst, the catalytic activity was improved to give the biaryls in 11.7% (with **2b**, entry 15) and 12.0% yield (with **2c**, entry 18). However, addition of an excess phen·H_2O to this system also discouraged the reaction (entry 19). The reaction was also catalyzed by [Pd(OAc){$C_6H_3(CO_2Me)_2$-2,3}(phen)] (**1d**) (entries 21-22). This catalysis never ever proceeded in the absence of a Pd catalyst (entries 23-25).

The time-course curve for the dehydrogenative coupling of **3** catalyzed by **1b**/**2b**·0.5H_2O at 200 ˚C under air showed an induction period and the biaryls yield plateaued around 6 h (Figure 6). However, when a combination of **1b**/**2a** was used as the catalyst, no induction period was observed with comparable yield under the same conditions. One of the possible explanations for this phenomenon is that [Cu(OAc)$_2$·H_2O] (**2a**) shows higher activity than [Cu(OAc)$_2$(phen)] (**2b**). Note that coordination of phen is indispensable for [Pd(OAc)$_2$] (**1a**) as shown in entry 3 in Table 2.

Table 2. Catalytic Dehydrogenative Coupling of Dimethyl Phthalate. [a]

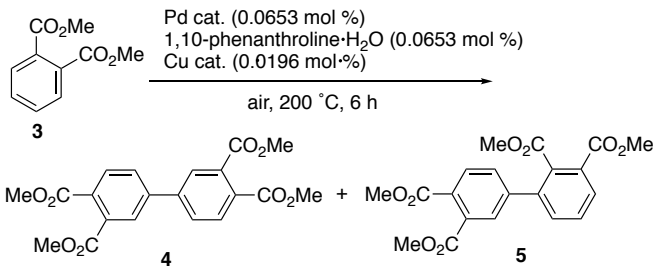

entry	Pd cat.	Cu cat.	yield/%	4/5	TON[b]	conv./%
1	1a	2a·H_2O	8.5	90/10	64	18.3
2[c]	1a	2a·H_2O	8.1	92/8	62	15.9
3[d]	1a	2a·H_2O	0.0		0	3.4
4	1a	2b·0.5H_2O	7.0	89/11	53	16.6
5	1a	2c	9.6	94/6	73	16.0
6	1a	2d	10.9	94/6	83	14.2
7	1a	none	1.9	94/6	14	6.2
8[d]	1b	2a·H_2O	6.3	89/11	48	15.9
9[e]	1b	2a·H_2O	7.2	91/9	55	15.7
10[d]	1b	2b·0.5H_2O	6.2	91/9	47	12.9
11[ef]	1b	2c	9.6	94/6	73	15.4
12[f]	1b	2c	3.7	93/7	28	10.8
13[d,]	1b	none	0.8	92/8	6	5.9
14[d]	1c	2a·H_2O	6.2	92/8	47	15.2
15[e]	1c	2a·H_2O	11.7	93/7	89	15.4
16[d]	1c	2b·0.5H_2O	9.7	92/8	75	13.5
17[e]	1c	2b·0.5H_2O	8.7	94/6	67	9.8
18[e]	1c	2c	12.0	94/6	91	12.7
19[f]	1c	2c	4.1	93/7	31	10.8
20[d]	1c	none	2.3	93/7	17	6.4
21[e]	1d	2a·H_2O	9.6	94/6	73	13.1
22[d]	1d	2b·0.5H_2O	8.3	94/6	64	12.1
23[d]	none	2a·H_2O	0.0		0	0.9
24[d]	none	2b·0.5H_2O	0.0		0	2.1
25	none	none	0.0		0	0.5

[a]Standard conditions: [Pd] = 4.00 mM (0.065 mol %), [**2a**·H_2O] = 1.20 mM (0.020 mol%), [phen·H_2O] = 4.00 mM (0.065 mol %), **3**: 25 mL. Air = 0.1 MPa, temp = 200 ˚C, time = 6 h. [b]TONs: turn over numbers. [c][phen· H_2O] = 5.20 mM. [d]without addition of PHEN. [e][phen·H_2O] = 1.20 mM. [f][phen·H_2O] = 5.20 mM.

In summary of this section, all Pd complexes **1a-d** catalyzed the dehydrogenative coupling of dimethyl phthalate.

Solid- and Solution-Phase XAFS Studies. The catalyst solution for the dehydrogenative arene coupling was studied by the XAFS analysis. We used a synchrotron radiation at SPring-8 BL01B1 beamline.[39] First of all we compared the XAFS spectra of **1b** in the crystalline solid-phase in a BN pellet[40] with the solution-phase in dimethyl phthalate (**3**).

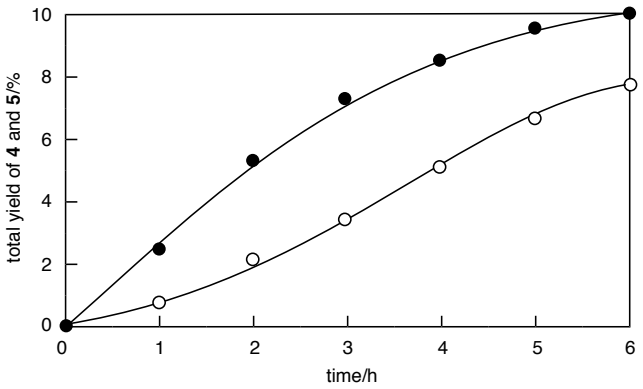

Figure 6. Time-yield curves for 1b/2b·0.5H_2O (1b = 0.0634 mol %, 2b·0.5H_2O = 0.0190 mol %) (open circles) and for 1b/2a·0.5H_2O (1b = 0.0635 mol %, 2a·0.5H_2O = 0.0173 mol %) (closed circles) at 200 ˚C under air in 3 (25 mL).

As shown in Figure 7, **1b** in **3** shows almost identical Pd K-edge (24.357 keV) XANES (X-ray absorption near edge structure) spectra, suggesting the Pd valency and basic geometry in a solution to be identical with the crystal structure.

Figure 8 shows the Pd K-edge solution-phase EXAFS (extended X-ray absorption fine structure) spectra of a mixture of **1a** and **2b** in **3**.

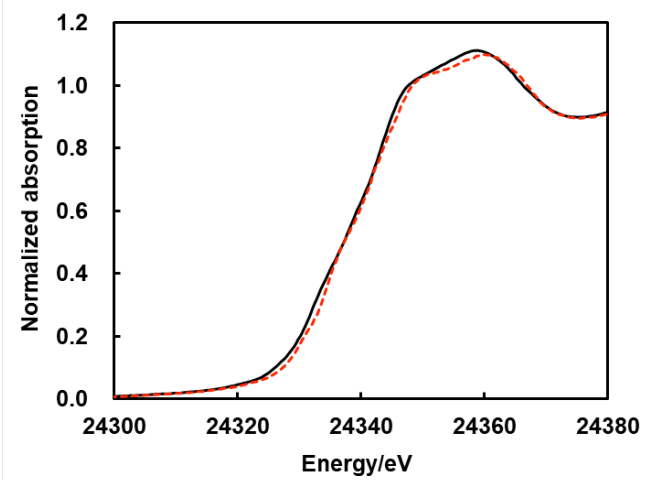

Figure 7. The Pd K-edge XANES spectra of 1b in solid-phase in BN pellet (black line) and solution-phase in 3 (red dotted line).

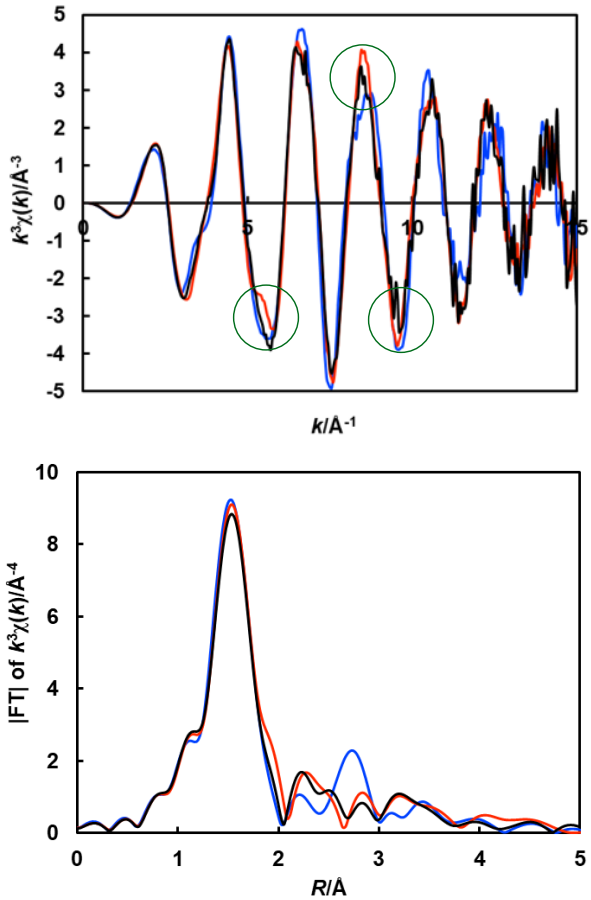

Figure 8. The Pd K-edge solution-phase EXAFS of 1a/2b·0.5H₂O in 3 (black), 1a (blue) and 1b (red) in 3 as the reference. The green circles in the k-space graph point major unconformities between 1a (black) and 1b (red).

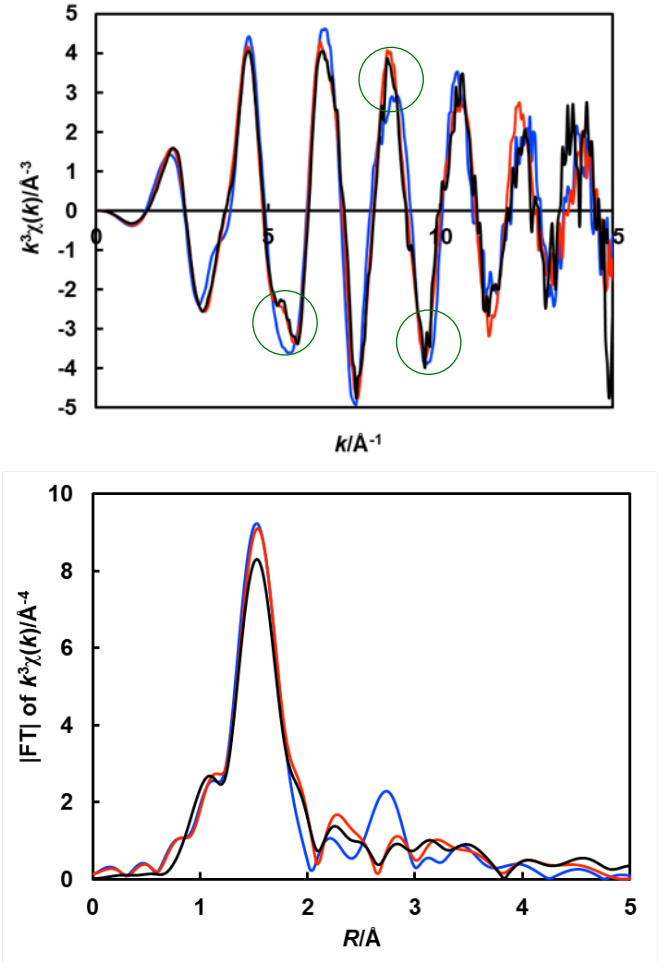

Figure 9. The Pd K-edge solution-phase EXAFS spectra after addition of phen·H₂O to a solution of 1a and 2b·0.5H₂O in 3 (black), 1a (blue) and 1b (red) as the reference. The green circles in the k-space graph highlighted conformities between 1a (black) and 1b (red).

The green circles in the *k*-space graph point major unconformities of the **1a**/**2b** (black line) and **1b** (red line). These data suggest that spontaneous migration of the phen ligand in **2b** to **1a** would insufficiently occur at room temperature.

Addition of phen·H_2O to the solution of **1a**/**2b** in **3** caused significant change in the solution-phase EXAFS spectrum and the resulting spectrum almost completely overlapped with **1b** (Figure 9). Accordingly, we have succeeded to confirm coordination of phen to **1a** and formation of **1b** by EXAFS.

Next, we have conducted the dehydrogenative coupling reaction of **3** catalyzed by **1a**/**2b**·0.5H_2O/phen·H_2O at 200 ˚C for 1 h under the atmosphere of oxygen (0.1 MPa), and measured the solution-phase XAFS of the catalytic solution to know the changes of the Pd species. In order to obtain sufficient Pd K-edge XAFS data, we performed the reaction under the higher catalyst concentrations [**1a** (25 mM), **2b**·0.5H_2O (7.5 mM), phen·H_2O (25 mM)] than the standard set of conditions. We stopped the catalysis after 1 h in order to observe the catalysis by XAFS. The catalysis gave the biaryl products in 3.3% (**4**/**5** = 95/5) suggesting 4 TONs by GLC analysis. Figure 10 shows the changes in the EXAFS before and after the reaction at 200 ˚C catalyzed by **1a**/**2b**·0.5H_2O /phen·H_2O . Similar catalyses for dehydrogenative coupling of **3** by **1c**/**2b**·0.5H_2O/phen·H_2O and **1d**/**2b**·0.5H_2O/phen·H_2O at 200 ˚C for 1 h produced the biaryls in 4.1% (**4**/**5** = 94/6) with 5 TONs, and 2.1% (**4**/**5** = 88/12) with 3 TONs, respectively (Figures 11 and 12). According to these EXAFS spectra (Figures 10-12), an almost identical Pd species was formed regardless of the starting Pd complexes **1a**, **1c** and **1d**. In fact, the merged EXAFS spectra of the catalytic solution starting from **1a**, **1c** and **1d** overlapped each other both in the *k*- and *R*-spaces (Figure 13). Notably no significant change was observed after the catalysis in the EXAFS spectra of **1c** and **1d**. The TONs for the **1c**/**2b**·0.5H_2O/phen·H_2O and **1d**/**2b**·0.5H_2O/phen·H_2O systems suggest that the catalyst

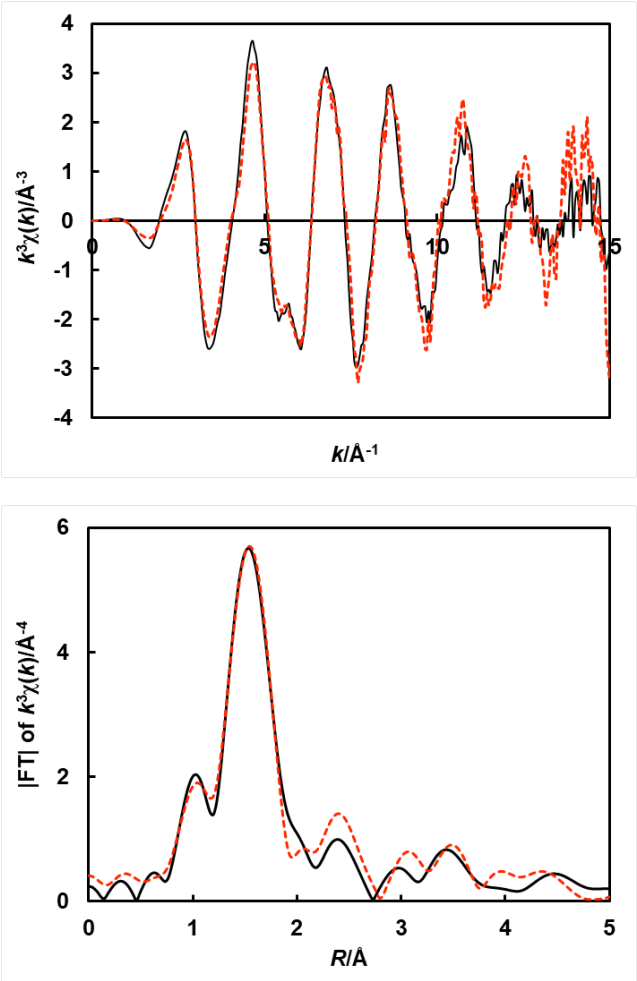

Figure 10. The Pd K-edge solution-phase EXAFS spectra of 1a/2b·0.5H$_2$O/phen·H$_2$O before (red dotted line) and after (black line) the catalysis.

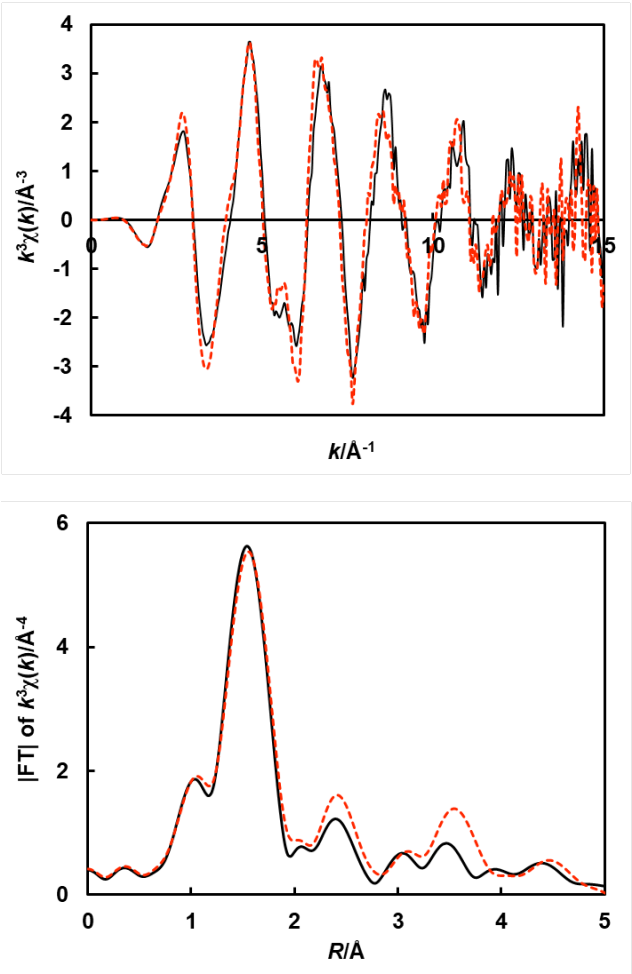

Figure 11. The Pd K-edge solution-phase EXAFS spectra of 1c/2b·0.5H$_2$O/phen·H$_2$O (red dotted line) before and after (black line) catalysis.

averagely goes through 5 and 3 catalytic cycles, respectively. Nevertheless, a slight difference was observed between them on the EXAFS peaks after the catalysis. Given the low reactivity of **1d** in the stoichiometric reaction, a certain amount of **1d** might remain unreacted after the catalysis in the **1d**/**2b**·0.5H$_2$O/phen·H$_2$O system.

Figure 14 shows the merged XANES spectra of after the catalyses in **3** catalyzed by **1a**/**2b**·0.5H$_2$O/phen·H$_2$O, and **1c**/**2b**·0.5H$_2$O/phen·H$_2$O, and **1d**/**2b**·0.5H$_2$O/phen·H$_2$O. These spectra clearly show the valency of the new species derived from **1a** in the catalysis is a divalent, which shows almost the same spectrum as **1c** and **1d**. Furthermore, an isosbestic point is found in these normalized XANES spectra at 24.341 keV. An isosbestic point generally shows transformation between two species either by the extent of reaction or the position of the equilibrium. However, given the resolution of XANES, the isosbestic point would suggest these constituents being mixed in different amount in the catalyst solution.[41]

For further considerations of these EXAFS spectra of the intermediate or resting state, we calculated the EXAFS spectra by the FEFF program[42] based on the optimized structures of **1c** and **1d** obtained by the DFT calculations. As shown in Figure 4, the optimized structures of **1c** and **1d** are very close to each other, and the differences between **1c** and **1d** for the bond distances of the Pd–C, Pd–N and Pd–O in the primary coordination sphere are only within 0.01 Å. Since resolution of the atomic distances by EXAFS is around 0.1 Å, the difference between **1c** and **1d** appears in the second coordination sphere and beyond. Figures 15 and 16 show the solution-phase EXAFS spectra of **1c** and **1d** and their FEFF calculation fits based on the optimized structures obtained by the DFT calculations (Figure 4).

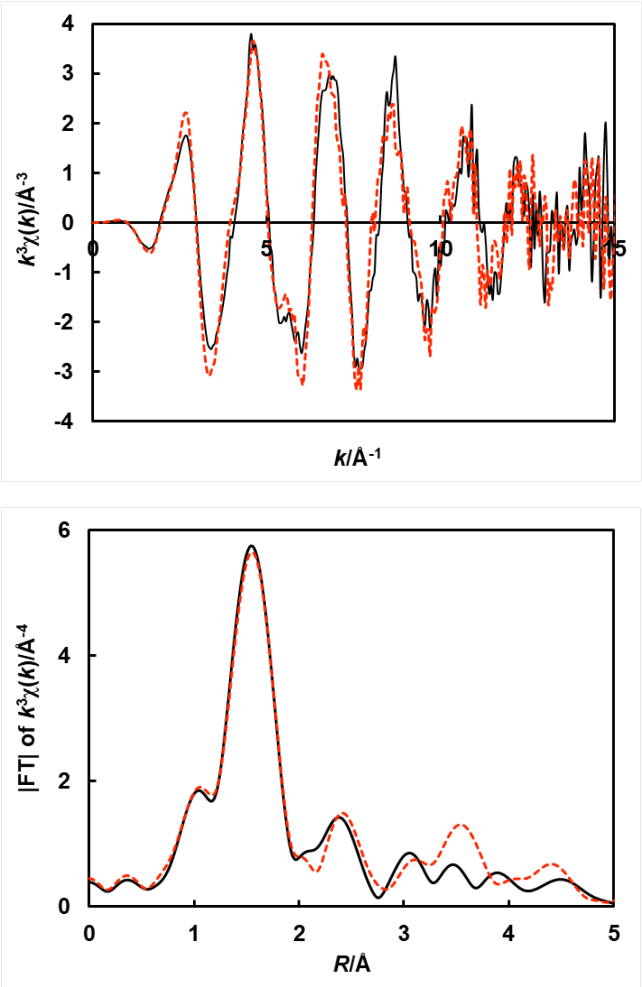

Figure 12. The Pd K-edge solution-phase EXAFS spectra of 1d/2b·0.5H_2O/phen·H_2O before (red dotted line) and after (black line)catalysis.

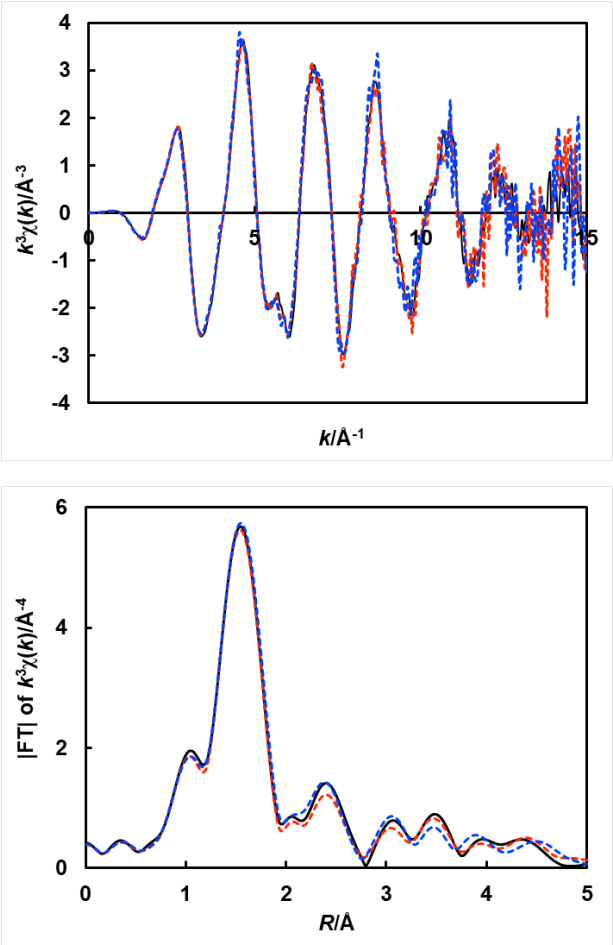

Figure 13. The solution-phase EXAFS spectra after catalyses in 3 starting from 1a/2b·0.5H_2O/phen·H_2O (black), 1c/2b·0.5H_2O/phen·H_2O (red dotted line) and 1d/2b·0.5H_2O/phen·H_2O (blue dotted line).

The *R*-factors for **1c** and **1d** are 0.0124 and 0.0137, respectively. These data suggest the intermediate or resting state after the catalysis also contains the acetato, phthalyl, and the phen ligand. However, the solution-phase EXAFS spectrum of the Pd species after the catalysis has a slight difference from **1c** or **1d** in the third coordination sphere and beyond. One of the possibilities is the presence of a Cu complex in the far side from the Pd center. In fact, Hosokawa, Murahashi and co-workers suggested formulation of Pd-Cu dinuclear species in the Wacker-type reactions,[43] and they obtained crystals of $[(dmf)_4Cl_2Cu\text{-}(PdCl_2)_2]_n$ in the $[PdCl_2]/[CuCl]/O_2$ catalyzed Wacker reaction in DMF.[44] However, we remain this issue for further study because we do not have any evidence for this point so far. An important conclusion achieved in the part of the EXAFS study is that a same species is eventually formulated regardless of the starting Pd catalysts **1a**, **1c** and **1d** as an intermediate or resting state. The fact that no significant change has been observed in the EXAFS spectrum after the catalysis for **1c** and **1d**, also suggests the [Pd(OAc)(dimethyl phthalyl)(phen)] structure basically remained intact. Therefore, we can conclude that [Pd(OAc)(dimethyl phthalyl)(phen)] species is surely produced from **1a** or **1b** during the catalysis.

Consistent Catalytic Cycle. These stoichiometric and catalytic reactions, and the XAFS data provide useful mechanistic insights and the catalytic cycle shown in Scheme 4 is consistent with all experimental data. The added PHEN immediately coordinates to $[Pd(OAc)_2]$ (**1a**) to give $[Pd(OAc)_2(phen)]$ (**1b**), which is confirmed by the EXAFS experiment. Then, heating of **1b** in dimethyl phthalate (**3**) produces **1c** and **1d** probably either by C–H

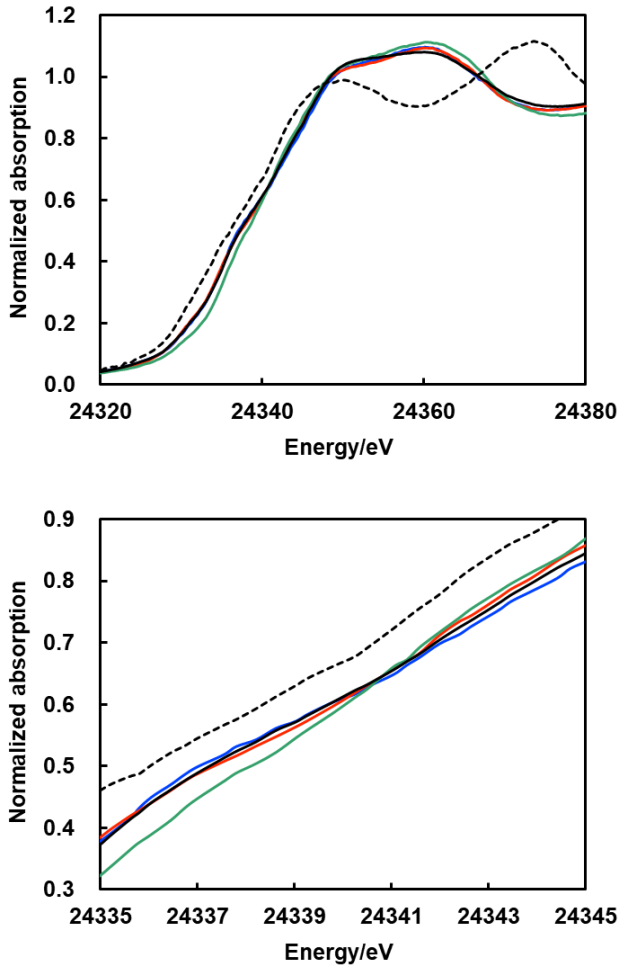

Figure 14. The Pd K-edge normalized solution-phase XANES spectra of 1a/2b·0.5H_2O/phen·H_2O in 3 (green), after the catalysis by 1a/2b·0.5H_2O/phen·H_2O in 3 (black), 1c (red) and 1d in 3 (blue). The dotted line shows a Pd foil. Spectra around edge jump region and spectra around the isosbestic point (bottom).

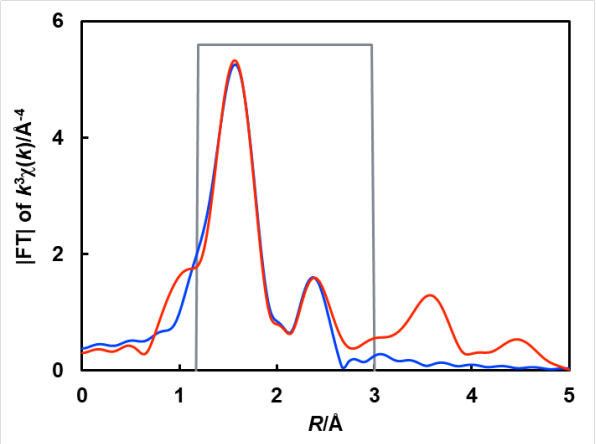

Figure 15. Solution-phase EXAFS spectra of 1c (red) and the FEFF-calculated fits based on the optimized structures obtained by the DFT calculations (blue). The FEFF fitting area is shown in the gray box.

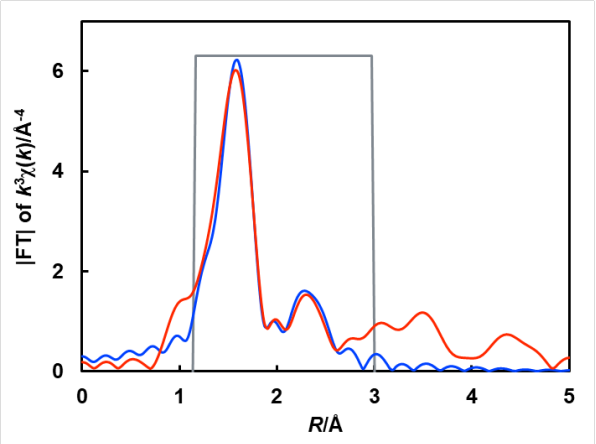

Figure 16. Solution-phase EXAFS spectra of 1d (red) and the FEFF-calculated fits based on the optimized structures obtained by the DFT calculations (blue). The FEFF fitting area is shown in the gray box.

bond activation through the IES mechanism[3] or electrophilic aromatic substitution. The reverse reactions, acidolyses of **1c** and **1d** with AcOH to **1b**, may connect among them. Although the second C–H bond activation of the coming **3** cannot be ruled out, present results show the presence of disproportionation of **1c** to give **1b** and **1f**, and subsequent reductive elimination releases **4**. Note that as can be seen in the stoichiometric reactions, a diarylpalladium(II) species is not stable and is prone to carry on subsequent reductive elimination. The reversible liberation of the acetato anion from **1c** may be responsible to this disproportionation. The oxidation of resulting **1g** occurs by **2a** to regenerates **1b**. On the other hand, reaction of **1b** with **3** also produces the regioisomer **1d**. While the disproportionation between **1c** and **1d** produces **5**, no disproportionation occurs between **1d** complexes. Because the present catalysis involves **1b**, **1c** and **1d** according to the XAFS analyses, **1c** and **1d** would be regarded as an active intermediate and resting state, respectively. The rate-determining step would be the disproportionation reaction.

■ CONCLUDING REMARKS

We elucidated the detailed mechanism for the dehydrogenative coupling of dimethyl phthalate catalyzed by [Pd(OAc)$_2$]/[Cu(OAc)$_2$]/phen system. The present catalysis involves [Pd(OAc){C_6H_3(CO_2Me)$_2$-3,4}(phen)] (**1c**) and [Pd(OAc){C_6H_3(CO_2Me)$_2$-2,3}(phen)] (**1d**), where disproportionation of **1c** is a consistent pathway to give tetramethyl 3,3'4,4'-biphenyltetracarboxylate (**4**). The

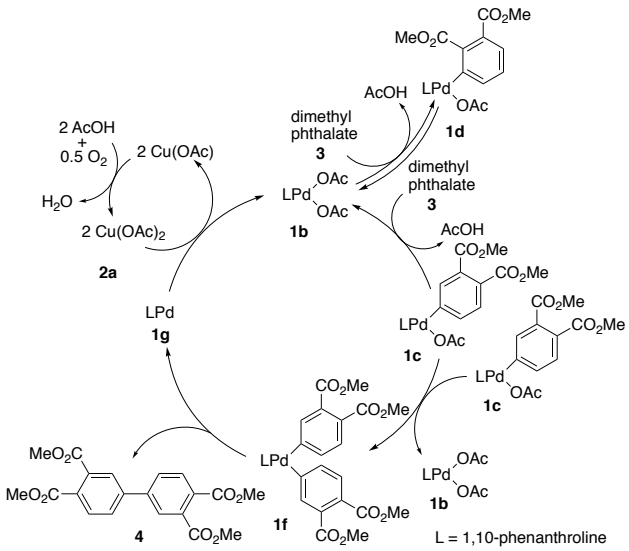

Scheme 4. A Proposed Catalytic Cycle for Dehydrogenative Coupling of Dimethyl Phthalate catalyzed by [Pd(OAc)$_2$]/[Cu(OAc)$_2$]/phen.

present solution-phase EXAFS data clearly suggests formation of **1c** and **1d** as intermediates or resting states in the catalysis. The mechanistic insights in copper cycle and possibility to form a Pd-Cu dinuclear species are further field to be solved.

■ EXPERIMENTAL SECTION

General Procedures. All procedures described in this paper were carried out under atmosphere except noted. Dimethyl phthalate (**3**), dimethyl adipate, and dichloromethane were used as received from commercial suppliers. Benzene, Et$_2$O and tetrahydrofuran (thf) were taken from a Glass Contour Ultimate Solvent Systems. 1,2-dichloroethane was used as received. Dmso-d_6 was dried over activated molecular sieves 4A and dichloromethane-d_2 and chloroform-d_1 were used as received. [Pd(OAc)$_2$] (**1a**), [Cu(OAc)$_2$·H$_2$O] (**2a**·H$_2$O), 1,10-phenanthroline·H$_2$O, and tmeda were used as received. [Pd(OAc)$_2$(phen)][24] (**1b**), [Pd(dba)$_2$][45] and [Cu(OAc)$_2$(phen)·0.5H$_2$O][33] (**2b**·0.5H$_2$O) were prepared according to literature methods. Dimethyl 4-bromophthalate,[46] dimethyl 3-iodophthalate,[47] dimethyl 4-(pinacolboryl)phthalate[48] and diethyl 4-pinacolboryl)phthalate[48] were prepared according to the modification of literature methods . ^{1}H and ^{13}C NMR spectra were recorded on a JEOL ECX-400P (400 MHz for ^{1}H). Chemical shifts (δ) are given in ppm, relative to TMS. All coupling constants are given in Hz. Elemental analyses were carried out on a Perkin-Elmer 2400 series II CHN analyzer. IR spectra were recorded on JASCO FT/IR-4100 with use of KBr disks. GLC analyses was performed on a Shimadzu GC-14B or GC2014 with FID detector equipped with InertCap 1 column (0.25 mm i.d. x 30 m). The GC-MS analyses were performed on a Shimadzu QP2010 with use of TC-1 column (0.25 mm i.d. x 30 m). A stoichiometric transmetallation was performed with a personal organic synthesizer EYELA ChemiStation PPM-5512. The ESI TOF-MS analysis was performed on a Bruker micrOTOF. The UV-vis analysis was performed on a Shimadzu MultiSpec 1500 with a photo-diode-alley detector. The catalyses were carried out with use of an EYELA SynFlex aluminum block heater system.

[PdBr{C$_6$H$_3$(CO$_2$Me)$_2$-3,4}(tmeda)]. Under a nitrogen atmosphere, [Pd(dba)$_2$] (2.8766 g, 5.0028 mmol) were placed in a Schlenk tube (250 mL), to which benzene (70 mL), tmeda (750 μL, 5.10 mmol) and dimethyl 4-bromophthalate (950 μL, 5.25 mmol) were added by a syringe or hypodermic syringe. The reaction mixture was warmed at 50 ˚C for 38.5 h to give a grayish green solid. After removal of the solution, the solid was washed with benzene (150 mL) to give [PdBr(C$_6$H$_3$(CO$_2$Me)$_2$-3,4)(tmeda)] in 70% yield (1.72345 g, 3.4767 mmol). This compound was characterized by ^{1}H NMR. ^{1}H NMR (400 MHz, CD$_2$Cl$_2$, r.t.): δ 2.39 (s, 6H, N*Me*), 2.56 (t, $^3J_{H-H}$ = 5.4 Hz, 2H, NC$_2$*H*$_4$N), 2.62 (s, 6H, N*Me*), 2.73 (t, $^3J_{H-H}$ = 5.4 Hz, 2H, NC$_2$*H*$_4$N), 3.79 (s, 3H, CO$_2$*Me*), 3.82 (s, 3H, CO$_2$*Me*), 7.33 (d, $^3J_{H-H}$ = 8.0 Hz, 1H, 6-C*H*), 7.50 (dd, $^3J_{H-H}$ = 8.0 Hz, $^4J_{H-H}$ = 1.7 Hz, 1H, 5-C*H*), 7.58 (d, $^4J_{H-H}$ = 1.7 Hz, 1H, 3-C*H*). ^{13}C{^{1}H} NMR (100.5 MHz, CD$_2$Cl$_2$, r.t.): δ 48.79 (s, tmeda), 50.96 (s, tmeda), 52.38 (s, CO$_2$*Me*), 52.53 (s, CO$_2$*Me*), 58.67 (s, tmeda), 63.04 (s, tmeda), 125.81 (s), 126.37 (s), 130.26 (s), 135.04 (s), 138.33 (s), 157.28 (s), 168.50 (s, *C*O$_2$Me), 169.47 (s, *C*O$_2$Me).

[PdBr{C$_6$H$_3$(CO$_2$Me)$_2$-3,4}(phen)]. [PdBr(C$_6$H$_3$(CO$_2$Me)$_2$-3,4)(tmeda)] (247.89 mg, 0.50007 mmol) and 1,10-phehtanthroline·H$_2$O (93.18 mg, 0.5168 mmol) were dissolved in thf (20 mL) and the reaction mixture was stirred at room temperature for 24 h to give a white precipitate. After removal of the solution, the white residue was washed with acetone and hexane. Removal of volatile matters gave white powder of [PdBr{C$_6$H$_3$(CO$_2$Me)$_2$-3,4}(phen)] in 89% yield (250.1 mg, 0.4468 mmol). ^{1}H NMR (400 MHz, CD$_2$Cl$_2$, r.t.): δ 3.84 (s, 3H, CO$_2$*Me*), 3.85 (s, 3H, CO$_2$*Me*), 7.50 (d, $^3J_{H-H}$ = 7.9 Hz, 1H, 3-C*H*), 7.67 (dd, $^3J_{H-H}$ = 8.2, 5.2 Hz, 1H, *phen*), 7.72 (dd, $^3J_{H-H}$ = 8.0 Hz, $^4J_{H-H}$ = 1.4 Hz, 1H, 2-C*H*), 7.79 (d, $^4J_{H-H}$ = 1.4 Hz, 1H, 6-C*H*), 7.92 (dd, $^3J_{H-H}$ = 8.2, 4.9 Hz, 1H, *phen*), 7.99 (AB, $^3J_{H-H}$ = 8.9 Hz, 1H, *phen*), 8.03 (AB, $^3J_{H-H}$ = 8.9 Hz, 1H, *phen*), 8.08 (dd, $^3J_{H-H}$ = 5.2 Hz, $^4J_{H-H}$ = 1.4 Hz, 1H, *phen*), 8.45-8.63 (m, 2H, *phen*), 9.58 (dd, $^3J_{H-H}$ = 4.9 Hz, $^4J_{H-H}$ = 1.6 Hz, 1H, *phen*). ^{13}C{^{1}H} NMR (100.5 MHz, CD$_2$Cl$_2$, r.t.): δ 52.51 (s, CO$_2$*Me*), 52.62 (s, CO$_2$*Me),* 125.90 (s), 126.48 (s), 127.14 (s), 127.26 (s), 127.88 (s), 130.08 (s), 130.47 (s), 130.95 (s), 138.45 (s), 138.61 (s), 138.72 (s), 145.39 (s), 147.44 (s), 150.94 (s), 151.00 (s), 157.13 (s), 168.53 (s, *C*O$_2$Me), 169.49 (s, *C*O$_2$Me).

[Pd(OAc){$C_6H_3(CO_2Me)_2$-3,4}(phen)] (1c). In a 50 mL round bottom flask, above solid (279.90 mg, 0.50008 mmol as [PdBr($C_6H_3(CO_2Me)_2$-3,4)(phen)]) was reacted with AgOAc (166.26 mg, 0.99611 mmol) in dichloromethane (20 mL) for 2.5 h at room temperature in the dark. A brown solid deposited from the reaction system. The insoluble solid was filtered off and the solution was evaporated to give a pale yellow solid, which was recrystallized from dichloromethane/hexane to give **1c** as pale yellow crystals in 50% yield (135.1 mg, 0.2515 mmol). ^{1}H NMR (400 MHz, CD_2Cl_2, 20.9 ˚C): δ 2.02 (s, 3H, OAc), 3.84 (s, 3H, 3H, CO_2*Me*), 3.85 (s, 3H, CO_2*Me*), 7.48 (d, $^3J_{H-H}$ = 7.9 Hz, 1H, 5-C*H*), 7.62 (dd, $^3J_{H-H}$ = 8.2, 5.2 Hz, 1H, *phen*), 7.82 (dd, $^3J_{H-H}$ = 7.9 Hz, $^4J_{H-H}$ = 1.4 Hz, 1H, 6-C*H*), 7.86 (d, $^4J_{H-H}$ = 1.4 Hz, 1H, 2-C*H*), 7.91 (dd, $^3J_{H-H}$ = 7.9, 5.2 Hz, 1H, *phen*), 7.98 (AB, $^3J_{H-H}$ = 13.6 Hz, 1H, *phen*), 8.02 (AB, $^3J_{H-H}$ = 13.6 Hz, 1H, *phen*), 8.26 (dd, $^3J_{H-H}$ = 5.2 Hz, $^4J_{H-H}$ = 1.4 Hz, 1H, *phen*), 8.53 (dd, $^3J_{H-H}$ = 8.3 Hz, $^4J_{H-H}$ = 1.4 Hz, 1H, *phen*), 8.55 (dd, $^3J_{H-H}$ = 8.3Hz, $^4J_{H-H}$ = 1.6 Hz, 1H, *phen*), 8.80 (dd, $^3J_{H-H}$ = 4.9 Hz, $^4J_{H-H}$ = 1.4 Hz, 1H, *phen*). ^{13}C{^{1}H} NMR (100.5 MHz, CD_2Cl_2, 21.7 ˚C): δ 23.78 (s, O*Ac*), 52.50 (s, CO_2*Me*), 52.61 (s, CO_2*Me*), 125.65 (s, C_6H_3), 125.80 (s, C_6H_3), 126.73 (s, C_6H_3), 126.79 (s, C_6H_3), 127.73 (s, C_6H_3), 130.03 (s, *phen*), 130.41 (s, *phen*), 130.66 (s, *phen*), 134.83 (s, *phen*), 135.49 (s, *phen*), 138.59 (s, *phen*), 144.94 (s, *phen*), 147.91 (s, *phen*), 149.56 (s, *phen*), 152.44 (s, *phen*), 149.85 (s, *phen*), 168.71 (s, *C*O_2Me), 169.59 (s, *C*O_2Me), 177.34 (s, O*Ac*). Anal. Calcd for $C_{24}H_{20}N_2O_6Pd$: C, 53.50; H, 3.74; N, 5.20. Found: C, 53.93; H, 4.16; N, 5.43.

[PdI{$C_6H_3(CO_2Me)_2$-2,3}(phen)] (1e). Treatment of [Pd(dba)$_2$] (996.0 mg, 1.403 mmol) with dimethyl 3-iodophthalate (640.4 mg, 2.001 mmol) and 1,10-phehtanthroline·H_2O (327.4 mg, 1.817 mmol) in benzene (20 mL) at 50 ˚C for 4 h gave yellow powder of **1e** in 78% yield (663.2 mg, 1.093 mmol). This compound was characterized with ^{1}H NMR and X-ray analysis (*vide infra*). ^{1}H NMR (400 MHz, CD_2Cl_2, r.t.): δ 3.65 (s, 3H, CO_2*Me*), 3.85 (s, 3H, CO_2*Me*), 7.19 (t, $^3J_{H-H}$ = 7.7 Hz, 1H, 5-C*H*), 7.56 (dd, $^3J_{H-H}$ = 7.6 Hz, $^4J_{H-H}$ = 1.1 Hz, 1H, 4- or 6-C*H*), 7.69 (dd, $^3J_{H-H}$ = 8.2, 5.2 Hz, 1H, *phen*), 7.83 (dd, $^3J_{H-H}$ = 7.7 Hz, $^4J_{H-H}$ = 1.1 Hz, 1H, 6- or 4-C*H*), 7.87 (dd, $^3J_{H-H}$ = 8.2, 4.9 Hz, 1H, *phen*), 7.90 (dd, $^3J_{H-H}$ = 5.2 Hz, $^4J_{H-H}$ = 1.4 Hz, 1H, *phen*), 7.98 (AB, $^3J_{H-H}$ = 8.9 Hz, 1H, *phen*), 8.01 (AB, $^3J_{H-H}$ = 8.9 Hz, 1H, *phen*), 8.52 (dd, $^3J_{H-H}$ = 2.8 Hz, $^4J_{H-H}$ = 1.5 Hz, 1H, *phen*), 8.54 (dd, $^3J_{H-H}$ = 2.9 Hz, $^4J_{H-H}$ = 1.4 Hz, 1H, *phen*), 9.83 (dd, $^3J_{H-H}$ = 4.9 Hz, $^4J_{H-H}$ = 1.5 Hz, 1H, *phen*).

[Pd(OAc){$C_6H_3(CO_2Me)_2$-2,3}(phen)] (1d). Treatment of **1e** (663.2 mg, 1.093 mmol) with AgOAc (184.1 mg, 1.103 mmol) for 4 h at room temperature in dichloromethane (70 mL) gave pale yellow powder of **1d** in 91% yield (536.4 mg, 0.9955 mmol). ^{1}H NMR (400 MHz, CD_2Cl_2, r.t.): δ 2.01 (s, 3H, O*Ac*), 3.65 (s, 3H, CO_2*Me*), 3.85 (s, 3H, CO_2*Me*), 7.21 (t, $^3J_{H-H}$ = 7.6 Hz, 1H, 4-C*H*), 7.58 (dd, $^3J_{H-H}$ = 8.2, 5.2 Hz, 1H, *phen*), 7.61 (d, $^3J_{H-H}$ = 8.9 Hz, 1H, 3- or 5-C*H*), 7.89 (dd, $^3J_{H-H}$ = 8.2, 4.9 Hz, 1H, *phen*), 7.95 (AB, $^3J_{H-H}$ = 8.9 Hz, 1H, *phen*), 8.00 (AB, $^3J_{H-H}$ = 8.9 Hz, 1H, *phen*), 8.04 (dd, $^3J_{H-H}$ = 7.6 Hz, $^4J_{H-H}$ = 1.1 Hz, 5- or 3-C*H*), 8.15 (dd, $^3J_{H-H}$ = 5.3 Hz, $^4J_{H-H}$ = 1.4 Hz, 1H, *phen*), 8.49 (dd, $^3J_{H-H}$ = 8.2 Hz, $^4J_{H-H}$ = 1.4 Hz, 1H, *phen*), 8.55 (dd, $^3J_{H-H}$ = 8.3 Hz, $^4J_{H-H}$ = 1.4 Hz, 1H, *phen*), 8.77 (dd, $^3J_{H-H}$ = 4.9 Hz, $^4J_{H-H}$ = 1.4 Hz, 1H, *phen*). ^{13}C{^{1}H} NMR (100.5 MHz, CD_2Cl_2, r.t.): δ 23.64 (s, O*Ac*), 52.27 (s, CO_2*Me*), 52.47 (s, CO_2*Me*), 125.26 (s), 125.65 (s), 127.24 (s), 127.49 (s), 128.07 (s), 129.98 (s), 130.18 (s), 138.33 (s), 128.40 (s), 139.91 (s), 141.03 (s), 145.14 (s), 147.75 (s), 149.59 (s), 151.23 (s), 153.28 (s), 167.63 (s, *C*O_2*Me*), 171.66 (s, *C*O_2Me), 177.34 (s, O*Ac*). Anal. Calcd for $C_{24}H_{20}N_2O_6Pd$·0.23CH_2Cl_2: C, 52.50; H, 3.74; N, 5.20. Found: C, 52.14; H, 3.59; N, 5.14. Note that including of 0.23 equiv of CH_2Cl_2 was confirmed by ^{1}H NMR.

Variable Temperature ^{1}H NMR Experiments of [Pd(OAc){$C_6H_3(CO_2Me)_2$-3,4}(phen)] (1c) and [Pd(OAc){$C_6H_3(CO_2Me)_2$-2,3}(phen)] (1d). (Complex **1c**): **1c** (5.60 mg, 0.0104 mmol) was dissolved in dmso-d_6 (0.6 mL). After measurement of the ^{1}H NMR spectrum, 1,10-phenanthroline·H_2O (2.02 mg, 0.0102 mmol) was added to the solution. Although resonances assignable to the free 1,10-phenanthroline broadened upon heating (30-80 ˚C), the degree of broadening of 1c was almost same as the variable temperature NMR without addition of 1,10-phenanthroline. ^{1}H NMR spectrum of **1c** (6.02 mg, 0.0112 mmol) in dmso-d_6 (0.6 mL) was measured at 30 ˚C. Then, NaOAc (1.31 mg, 0.0160 mmol) was added in the NMR tube. The variable temperature ^{1}H NMR spectra were measured in the range 30-90 ˚C. (Complex **1d**): **1d** (2.70 mg, 0.00501 mmol) was dissolved in dmso-d_6 (0.6 mL). After measurement of the ^{1}H NMR spectrum, 1,10-phenanthroline·H_2O (1.01 mg, 0.00510 mmol) was added to the solution. In the range 30-90 ˚C, no broadening was observed. Similar experiment of **1d** (2.92 mg, 0.00542 mmol) in the presence of NaOAc (1.96 mg, 0.0239 mmol) in the same temperature range was also performed.

Reactions of [Pd(OAc){$C_6H_3(CO_2Me)_2$-3,4}(phen)] (1c) and [Pd(OAc){$C_6H_3(CO_2Me)_2$-2,3}(phen)] (1d) with Acetic Acid. (Complex **1c**): An acetic acid (1.0 mL) solution of **1c** (27.33 mg, 0.05072 mmol) was heated at 100 ˚C for 30 min. After removal of acetic acid, CD_2Cl_2, CD_3OD and triphenylmethane (10.12 mg, 0.4142 mmol) as an internal standard were added. The ^{1}H NMR spectrum showed formation of [Pd(OAc)$_2$(phen)] (**1b**) in 98% yield (0.0497 mmol) along with dimethyl phthalate (**3**) in 78% (0.0395 mmol). (Complex **1d**): Similar treatment of **1d** (26.95 mg, 0.05001 mmol) gave [Pd(OAc)$_2$(phen)] (**1b**) in 96% yield (0.0482 mmol) with dimethyl phthalate (**3**) in 87% yield (0.0435 mmol).

Pyrolysis of [Pd(OAc){$C_6H_3(CO_2Me)_2$-3,4}(phen)] (1c). A solution of dimethyl adipate (0.5 mL) of **1c** (27.97 mg, 0.05005 mmol) was heated at 180 ˚C for 1 h. Then,

triphenylmethane (2.53 mg) was added as an internal standard. The ^{1}H NMR spectrum suggested formation of **4** in 60% yield (0.01508 mmol).

Pyrolysis of [Pd(OAc){$C_6H_3(CO_2Me)_2$-2,3}(phen)] (1d). Similar to the procedure in 4-6-1, treatment of **1d** (27.97 mg, 0.05005 mmol), dimethyl adipate (0.7 mL) at 180 ˚C for 8 h produced only dimethyl phthalate (**3**) in 10.2% and no formation of **4**, **5**, or tetramethyl 2,2',3,3'-biphenyltetracarboxylate (**6**) was observed.

Pyrolysis in the presence of [Pd(OAc){$C_6H_3(CO_2Me)_2$-3,4}(phen)] (1c) and [Pd(OAc){$C_6H_3(CO_2Me)_2$-2,3}(phen)] (1d). A solution of dimethyl adipate (1.0 mL) of **1c** (13.48 mg, 0.02502 mmol) and **1d** (13.48 mg, 0.02502 mmol) was heated at 180 ˚C for 8 h. Then, triphenylmethane (2.49 mg) was added to the solution as an internal standard. After dilution of the reaction mixture with thf, the GLC analysis suggested total yield of **4** and **5**: 25.0%, **4**/**5** ratio: 86/14, yield of **3**: 11.8%. Formation of tetramethyl 2,2',3,3'-biphenyltetracarboxylate was not observed.

Treatment of [PdBr{$C_6H_3(CO_2Me)_2$-3,4}(phen)] with $AgBF_4$. In acetone: [PdBr{$C_6H_3(CO_2Me)_2$-3,4}(phen)] (55.99 mg, 0.1000 mmol) was treated with $AgBF_4$ (46.35 mg, 0.2381 mmol) in the presence of biphenyl (15.47 mg, 0.1003 mmol) as an internal standard in acetone (5 mL) at room temperature for 24 h in the dark. The GLC analysis showed no formation of **4** and **5**. In dichloromethane: A similar treatment of [PdBr{$C_6H_3(CO_2Me)_2$-3,4}(phen)] (55.98 mg, 0.1000 mmol) with $AgBF_4$ (46.04 mg, 0.2365 mmol) in dichloromethane at room temperature for 4 days gave **4** in 21% yield (0.0106 mmol). Compound **5** was not observed at all.

Treatment of [PdI{$C_6H_3(CO_2Me)_2$-2,3}(phen)] (1e) with $AgBF_4$. Complex **1e** (24.27 mg, 0.04000 mmol) was treated with $AgBF_4$ (25.9 mg, 0.133 mmol) and biphenyl (10.04 mg, 0.06511 mmol) as an internal standard in **3** (2 mL) at room temperature for 24 h. No formation of **4**, **5** or **6** was observed.

Reactions of [PdX{$C_6H_3(CO_2Me)_2$}(phen)] with Dialkyl 4-(pinacolboryl)phthalate. [PdBr{$C_6H_3(CO_2Me)_2$-3,4}(phen)]: [PdBr{$C_6H_3(CO_2Me)_2$-3,4}(phen)] (5.70 mg, 0.0102 mmol), dimethyl 4-(pinacolboryl)phthalate (3.54 mg, 0.0111 mmol) and Ag_2O (4.84 mg, 0.0209 mmol) were placed in an NMR tube, to which CD_2Cl_2 was introduced. After 13 days at room temperature, I_2 (8.12 mg, 0.0320 mmol) was added to the reaction mixture. Based on dimethyl sulfone as an internal standard (1.03 mg, 0.0109 mmol), the yield of **4** was estimated to be 43% by GLC. Compound **5** was not observed at all. [Pd(OAc){$C_6H_3(CO_2Me)_2$-3,4}(phen)] (**1c**): **1c** (5.91 mg, 0.0110 mmol) reacted with dimethyl 4-(pinacolboryl)phthalate (3.42 mg, 0.0108 mg) and Ag_2O (4.84 mg, 0.0209 mmol) in CD_2Cl_2 at room temperature for 25 days to give **4** in 53% yield. [PdI{$C_6H_3(CO_2Me)_2$-2,3}(phen)] (**1e**): **1e** (6.11 mg, 0.0101 mmol) reacted with dimethyl 4-(pinacolboryl)phthalate (3.22 mg, 0.0101 mmol) and Ag_2O (4.78 mg, 0.0206 mmol) in CD_2Cl_2 at room temperature for 10 days but **5** was not observed. A similar treatment of **1c** (5.39 mg, 0.0100 mmol) with diethyl (4-pinacolboryl)phthalate (3.55 mg, 0.0102 mmol) and Ag_2O (4.66 mg, 0.0201 mmol) in 1,2-dichloroethane at 50 ˚C for 7 days produced 3,4-diethyl-3',4'-dimethyl 3,3',4,4'-biphenyltetracarboxylate (**7**) in 42% along with small amount of **4** in 2%. In this reaction, because resonances of **7** heavily overlapped with reactants in ^{1}H NMR and pure **7** was not available, we postulated the relative intensity for **7** in GLC analysis to be the same as **4** based on biphenyl as an internal standard. Formation of **7** was also confirmed with the GC-MS analysis.

Catalytic Dehydrogenative Coupling of Dimethyl Phthalate. Typical catalysis was carried out as follows: On a four-necked round bottle flask, a reflux condenser, gas inlet, thermometer and a stopper were installed. Then, [$Pd(OAc)_2$] (**1a**) (22.46 mg, 0.1000 mmol), [$Cu(OAc)_2 \cdot H_2O$] (**2a**·H_2O) (5.45 mg, 0.0300 mmol), phen·H_2O (19.82 mg, 0.09998 mmol), and dimethyl phthalate (**3**) (25.0 mL, 157.8 mmol) were added to the flask. Air stream was passed through the solution by use of a mini-compressor and the reaction system was heated at 200 ˚C for 6 h with magnetic stirring at the rate of 460 rpm. The products were estimated by an internal standard method using triphenylmethane, GLC analysis showed total yield of **4** and **5** in 9.7%, TON: 75, **4**/**5** ratio: 94/6, conversion: 12.0% and yield of methyl benzoate: 0.1%.

Time-course Curves for the Dehydrogenative Coupling of 3 Catalyzed by 1b/2b and 1b/2a. **1b**/**2b**: In a four-necked round bottom flask, **1b** (40.44 mg, 0.1001 mmol) and **2b**·0.5H_2O (10.84 mg, 0.02996 mmol) were added in **3** (25.0 mL, 157.8 mmol). Air stream was passed through the solution and the system was heated at 200 ˚C at the stirring rate of 460 rpm. When the temperature reached at 200 ˚C, we set the start time for the catalysis and the progress of the catalysis was monitored the reaction for every 1 h by GLC. Finally, triphenylmethane (24.31 mg) as an internal standard and THF were added to the solution. **1b**/**2a**·H_2O: **1b** (40.47 mg, 0.1002 mmol), **2a**·H_2O (5.43 mg, 0.0273 mmol) in **3** (25.0 mL, 157.8 mmol) at 200 ˚C for 6 h. The reaction was monitored for every 1 h by GLC.

Solid and Solution-Phase XAFS Measurements. Pd K-edge (24.357 keV) XANES and EXAFS measurements were carried out at the BL01B1 beamline at SPring-8 of the Japan Synchrotron Radiation Research Institute (JASRI). The measurements were performed at room temperature. A Si(311) two-crystal monochromater was used. The Pd K-edge XAFS data were collected by the transmission mode. The X-ray energy was calibrated using a Pd-foil, and the data analysis was performed with Athena in Demeter software package for Windows (ver.

0.9.25).[42] The BN pellets (*ca.* 0.5 mm thickness) were prepared for the solid-phase XAFS by mixing the Pd complex with commercial BN powder for dilution. For solution-phase XAFS, the catalyst solution in dimethyl phthalate (**3**) as a solvent were filtrated through a PTFE membrane filter with a 0.2 μm pore size.

Catalyses for XAFS Studies. (Entry 1) [$Pd(OAc)_2$] (**1a**) (25 mM), [$Cu(OAc)_2(phen)\cdot 0.5H_2O$] ([**2b**$\cdot 0.5H_2O$] (7.5 mM) and [phen$\cdot H_2O$] (25 mM) in dimethyl phthalate (**3**) at 200˚C for 1 h under oxygen. Total yield of **4** and **5**: 3.3%, TON: 4, **4**/**5** ratio: 95/5. Conversion: 7.5%, Yield of methyl benzoate: 0.6%. (Entry 2) [$Pd(OAc)\{C_6H_3(CO_2Me)_2\text{-}3,4\}(phen)$] (**1c**) (25 mM), [**2b**$\cdot 0.5H_2O$] (7.5 mM) in dimethyl phthalate at 200 ˚C for 1 h under oxygen. Total yield of **4** and **5**: 4.1%. TON: 5. **4**/**5** ratio: 94/6. Conversion: 8.5%. Yield of methyl benzoate: 0.4 %. (Entry 3) [$Pd(OAc)\{C_6H_3(CO_2Me)_2\text{-}2,3\}(phen)$] (**1d**) (25 mM), [**2b**$\cdot 0.5H_2O$] (7.5 mM) in dimethyl phthalate at 200 ˚C for 1 h under oxygen. Total yield of **4** and **5**: 2.1%. TON: 3. **4**/**5** ratio: 88/12. Conversion: 7.9%. Yield of methyl benzoate: 0.5%.

DFT Calculations of 1c and 1d. The density functional theory (DFT) calculations were employed with B3LYP. The basis set was consisted of the Stuttgarte Dresden SDD effective core potential basis set on the Pd atom and the 6-31G(d) basis sets on all other atoms. Effect of methyl benzoate as a solvent was included in the calculations by using the Polarizable Continuum Model (PCM).

FEFF Fitting Analysis for EXAFS. The fitting calculations were performed on FEFF6 program embedded with Artemis software,[42] where the theoretical scattering paths were generated from the DFT calculations of **1c** and **1d**.

Single Crystal X-ray Structure Analyses. Single crystals of **1b**, **1c**, **1e**, **2b** and **4** were selected by a polarized optical microscope. The selected crystals suitable for single crystal X-ray structure analysis were mounted on the top of a glass capillary with use of Paraton N® oil. A Rigaku AFC-7R Mercury II diffractometer with graphite-monochromated Mo Kα radiation (λ = 0.71075 Å) was used for data collection at 200 K. The collected data were solved by direct methods and refined by a full-matrix least-squares procedure using the CrystalStructure program (ver. 4.2).[49,50] All hydrogen atoms were treated as a riding model. The POV-Ray program (ver. 3.6.2) was used for depiction of the molecules.[51] CCDC 1813927, 1813928, and 1813930 contain the supplementary crystallographic data for **1c**, **1e** and **4**, respectively.

■ ASSOCIATED CONTENT

Supporting Information

The Supporting Information is available free of charge on the ACS Publications website at DOI: 10.1021/xxxxxx.

NMR data of new complexes [$PdBr\{C_6H_3(CO_2Me)_2\text{-}3,4\}(tmeda)$], [$PdBr\{C_6H_3(CO_2Me)_2\text{-}3,4\}(phen)$], **1c**, **1d**, **1e**, variable temperature NMR data for **1c** and **1d**, GLC and GC-MS charts for the reaction of **1c** with diethyl 4-(pinacolboryl)phthalate, Cartesian coordinates for **1c** and **1d** by DFT calculations, and FEFF parameters for **1c** and **1d** (PDF)

Accession Codes

CCDC 1813927-1813928 and 1813930 contain the supplementary crystallographic data for this paper. These data can be obtained free of charge via www.ccdc.cam.ac.uk/data_request/cif, or by emailing data_request@ccdc.cam.ac.uk, or by contacting The Cambridge Crystallographic Data Centre, 12 Union Road, Cambridge CB2 1EZ, UK; fax:+44 1223 336033.

■ AUTHOR INFORMATION

Corresponding Authors

*E-mail for M.H.: hrc@cc.tuat.ac.jp.
*E-mail for T.M.: mitsudom@cheng.es.osaka-u.ac.jp.
*E-mail for H.T.: takaya@scl.kyoto-u.ac.jp.

ORCID

Masafumi Hirano: 0000-0001-7835-1044

Nobuyuki Komine: 0000-0003-1744-695X

Zen Maeno: 0000-0002-9300-219X

Hikaru Takaya:0000-0003-4688-7842

Present Address

[§] Institute for Catalysis, Hokkaido University, N-21, W-10, Sapporo 001-0021, Japan.

Notes

The Authors declare no competing financial interest.

Author Contributions

The manuscript was written through contributions of all authors.

Funding Sources

Grant-in-Aid for Scientific Research on Innovative Areas, "3D Active-Site Science" 26105003.

■ ACKNOWLEDGMENT

We are grateful to Dr. Sayori Kiyota for elemental analyses. We thank Dr. Tetsuo Honma at JASRI for facilitation in SPring-8. M.H also thank Prof. Kotohiro Nomura at Tokyo Metropolitan University for fruitful discussion. This study was financially supported by Grant-in-Aid for Scientific Research on Innovative Areas, "3D Active-Site Science" 26105003.

ABBREVIATIONS

bpy: 2,2'-bipyridine ($C_{10}H_8N_2$). cod: cyclooctadiene (C_8H_{12}). dba: dibenzylidene acetone ($C_{17}H_{14}O$). phen: 1,10-phenanthroline ($C_{12}H_8N_2$). pin: pinacolyl ($C_6H_{12}O_2$). tmeda: tetramethylethylenediamine ($C_6H_{16}N_2$). TON (turn over number).

REFERENCES AND NOTE

(1) Itatani, H.; Yoshimoto, H. Palladium-catalyzed Synthesis of Aromatic Coupling Compounds. *Chem. Ind.* **1971**, 674-675.

(2) Shiotani, A.; Itatani, H.; Inagaki, T. Selective Coupling of Dimethyl Phthalate with Palladium Catalysts at Atmospheric Pressure. *J. Mol. Catal.* **1986**, 34, 57-66.

(3) This mechanism is also called as the concerted metalation-deprotonation (CMD) mechanism or the ambiphilic metal-ligand activation (AMLA).

(4) (a) Biswas, B.; Sugimoto, M.; Sakaki, S. C-H Bond Activation of Benzene and Methane by $M(\eta^2\text{-}O_2CH)_2$ (M = Pd or Pt). A Theoretical Study. *Organometallics* **2000**, *19,* 3895-3908. (b) Moritani, I.; Fujiwara, Y. Aromatic Substitution of Styrene-Palladium Chloride Complex. *Tetrahedron Lett.* **1967**, *8*, 1119-1122. (c) Davies, D. L.; Donald, S. M. A.; Macgregor, S. A. Computational Study of the Mechanism of Cyclometalation by Palladium Acetate. *J. Am. Chem. Soc.* **2005**, *127*, 13754-13755.

(5) (a) Davies, D. L.; Donald, S. M. A.; Al-Duaij, O.; Macgregor, S. A.; Pölleth, M. Electrophilic C-H Activation at Cp*Ir: Ancillary-Ligand Control of the Mechanism of C-H Activation. *J. Am. Chem. Soc.* **2006**, *128*, 4210-4211. (b) Boutadla, Y.; Davies, D. L.; Macgregor, S. A.; Poblador-Bahamonde, A. I. Mechanisms of C-H Bond Activation: Rich Synergy between Computation and Experiment. *Dalton Trans.* **2009**, 5820-5831. (c) Boutadla, Y.; Davies, D. L.; Macgregor, S. A.; Poblador-Bahamonde, A. I. Computational and Synthetic Studies on the Cyclometalation Reaction of Dimethylbenzylamine with $[IrCl_2Cp^*]_2$: Role of the Chelating Base. *Dalton Trans.* **2009**, 5887-5893.

(6) Oxgaard, J.; Tenn III, W. J.; Nielsen, R. J.; Periana, R. A.; Goddard III, W. A. Mechanistic Analysis of Iridium Heteroatom C-H Activation: Evidence for an Internal Electrophilic Substitution Mechanism. *Organometallics* **2007**, *26*, 1565-1567. (b) Ess, D. H.; Nielsen, R. J.; Goddard III, W. A.; Periana, R. A. Transition-State Charge Transfer Reveals Electrophilic, Ambiphilic, and Nucleophilic Carbon-Hydrogen Bond Activation. *J. Am. Chem. Soc.* **2009**, *131*, 11686-11688.

(7) (a) Laponte, D.; Fagnou, K. Overview of the Mechanistic Work on the Concerted Metallation-Deprotonation Pathway. *Chem. Lett.* **2010**, *39*, 1118-1126. (b) Gorelsky, S. I. Reactivity and Regioselectivity of Palladium-catalyzed Direct Arylation in Noncoorperative and Cooperative Processes. *Organometallics* **2012**, *31*, 4631-4634. (c) Raybov, A. D. Mechanisms of Intramolecular Activation of Carbon-Hydrogen Bonds in Transition-Metal Complexes. *Chem. Rev.* **1990**, *90*, 403-424.

(8) Tan, Y.; Barrios-Landeros, F.; Hartwig, J. F. Mechanistic Studies on Direct Arylation of Pyridine *N*-Oxide: Evidence for Cooperative Catalysis between Two Distinct Palladium Centers. *J. Am. Chem. Soc.* **2012**, *134*, 3683-3686.

(9) (a) Wakioka, M.; Nakamura, Y.; Hihara, Y.; Ozawa, F.; Sakaki, S. Factors Controlling the Reactivity of Heteroarenes in Direct Arylation with Arylpalladium Acetate Complexes. *Organometallics* **2013**, *32*, 4423-4430. (b) Wakioka, M.; Nakamura, Y.; Wang, Q.; Ozawa, F. Direct Arylation of 2-Methylthiophene with Isolated $[PdAr(\mu\text{-}O_2CR)(PPh_3)]_n$ Complexes: Kinetics and Mechanism. *Organometallics* **2012**, *31*, 4810-4816.

(10) (a) Izawa Y.; Stahl, S. S. Aerobic Oxidative Coupling of *o*-Xylene: Discovery of 2-Fluoropyridine as a Ligand to Support Selective Pd-catalyzed C-H Functionalization. *Adv. Synth. Catal.* **2010**, *352*, 3223-3229. (b) Wang, D.; Izawa, Y.; Stahl, S. S. Pd-Catalyzed Aerobic Oxidative Coupling of Arenes: Evidence for Transmetalation between Two Pd(II)-Aryl Intermediates. *J. Am. Chem. Soc.* **2014**, *136*, 9914-9917. (c) Wang, D.; Stahl, S. S. Pd-Catalyzed Aerobic Oxidative Biaryl Coupling: Non-Redox Co-catalysis by $Cu(OTf)_2$ and Discovery of $Fe(OTf)_3$ as a Highly Effective Cocatalyst. *J. Am. Chem. Soc.* **2017**, *139*, 5704-5707. (d) Wang, D.; Weinstein, A. B.; White, P. B.; Stahl, S. S. Ligand-Promoted Palladium-catalyzed Aerobic Oxidation Reactions. *Chem. Rev.* **2018**, *118*, 2636-2679.

(11) Stults, B. R.; Friedman, R. M.; Koenig, K.; Knowles, W.; Greegor, R. B.; Lytle, F. W. Homogeneous Asymmetric Catalysis: Structural Studies of Catalytic Intermediates using Extended X-ray Absorption Fine Structure. *J. Am. Chem. Soc.* **1981**, *103*, 3235-3237.

(12) Ti: Blanco-brieva, G.; Capel-sanchez, M. C.; Campos-martin, J. M.; Ferro, J. L. G.; Lede, E. J.; Adrini, L.; Requejo, F. G. Titanium K-edge XANES Analysis to Unravel the Local Structure of Alkene Epoxidation Titanium-Polysiloxane Homogeneous Catalysts. *Adv. Synth. Catal.* **2003**, *345*, 1314-1320.

(13) V: (a) Nomura, K.; Mitsudome, T.; Igarashi, A.; Nagai, G.; Tsutsumi, K.; Ina, T.; Omiya, T.; Takaya, H.; Yamazoe, S. Synthesis of (Adamantylimido)vanadium(V) Dimethyl Complex Containing (2-Anilidomethyl)pyridine Ligand and Selected Reactions: Exploring the Oxidation State of the Catalytically Active Species in Ethylene Dimerization. *Organometallics* **2017**, *36*, 530-542. (b) Nomura, K.; Oshima, M.; Mitsudome, T.; Harakawa, H.; Hao, P.; Tsutsumi, K.; Nagai, G.; Ina, T.; Takaya, H.; Sun, W.-H.; Yamazoe, S. Synthesis of Structural Analysis of (Imido)vanadium Dichloride Complexes Containing 2-(2'-Benz-imidazoyl)pyridine Ligands: Effect of Al Cocatalyst for Efficient Ethylene (Co)polymerization. *ACS Omega*, **2017**, *2*, 8660-8673.

(14) Cr: Moulin, J. O.; Evans, J.; McGuinness, D. S.; Reid, G.; Rucklidge, A. J.; Tooze, R. P.; Tromp, M. Probing the Effects of Ligand Structure on Activity and Selectivity of Cr(III) Complexes for Ethylene Oligomerization and Polymerization. *Dalton Trans.* **2008**, 1177-1127.

(15) Mo: Bartlett, S. A.; Wells, P. P.; Nachtegaal, M.; Dent, A. J.; Cibin, G.; Reid, G.; Evans, J.; Tromp, M. Insights in the Mechanism of Selective Olefin Oligomerization Catalysis using Stopped-Flow Freeze-Quench Techniques: A Mo K-edge QEXAFS Study. *J. Catal.* **2011**, *284*, 247-258.

(16) Mn: Feth, M. P.; Bolm, C.; Hildebrand, J. P.; Köhler, M.; Beckmann, O.; Bauer, M.; Ramamonjisoa, R.; Bertagnolli, H. Structural Investivation of High-valent Manganese-Salene Complexes by UV/Vis, Raman, XANES, and EXAFS Spectroscopy. *Chem. Eur. J.* **2003**, *9*, 1348-1359.

(17) Fe: (a) Bauer, M.; Gastl, C. X-Ray Absorption in Homogeneous Catalysis Research: The Iron-Catalyzed Michael Addition Reaction by XAS, RIXS and Multi-Dimensional Spectroscopy. *Phys. Chem. Chem. Phys.* **2010**, *12*, 5575-5584. (b) Schoch, R.; Desens, W.; Werner, T.; Bauer, M. X-Ray Spectroscopic Verification of the Active Species in Iron-Catalyzed Cross-Coupling Reactions. *Chem. Eur. J.* **2013**, *19*, 15816-15821. (c) Takaya, H.; Nakajima, S.; Nakagawa, N.; Isozaki, K.; Iwamoto, T.; Imayoshi, R.; Gower, N. J.; Adak, L.; Hatakeyama, T.; Honma, T.; Takagaki, M.; Sunada, Y.; Nagashima, H.; Hashizume, D.; Takahashi, O.; Nakamura, M. Inverstigation of Organoiron Catalysis in Kumada-Tamao-Corrium-Type Cross-Coupling Reaction Assisted by Solution-Phase X-ray Absorption Spectroscopy. *Bull. Chem. Soc. Jpn.* **2015**, *88*, 410-418.

(18) Ru: Rohr, M.; Grunwaldt, J.-D.; Baiker, A. Formylation with Supercritical Carbon Dioxide over Ru/Al_2O_3 Modified by Phosphines: Heterogeneous or Homogeneous Catalysis?. *J. Catal.* **2005**, *229*, 144-153.

(19) Ni: (a) Asakura, H.; Shishido, T.; Tanaka, T. In Situ Time-Resolved XAFS Study of the Reaction Mechanism of Bromobenzene Homocoupling Mediated by [Ni(cod)(bpy)]. *J. Phys. Chem. A* **2012**, *116*, 4029-4034. (b) Andrews, P.; Corker, J. M.; Evans, J.; Webster, M. Highly Active Homogenous Nickel Catalysts for Alkene Dimerization: Crystal Structure of $[Ni(\eta^3\text{-}C_3H_5)(PPh_3)Br]$ and In Situ Characterization of $AlEt_3$-Activated $[Ni(\eta^3\text{-}C_3H_3)(PPh_3)Br]$ by Nuclear Magnetic Resonance and Extended

X-ray Absorption Fine Structure Spectroscopy. *J. Chem. Soc., Dalton Trans*. **1994**, 1337-1347.

(20) Pd: (a) Tromp, M.; van Bokhoven, J. A.; van Haaren, R. J.; van Strijdonck, G. P. F.; van der Eerden, A. M. J.; van Leeuwen, P. W. N. M.; Koningsberger, D. C. Structure-Performance Relations in Homogeneous Pd Catalysis by In Situ EXAFS Spectroscopy. *J. Am. Chem. Soc*. **2002**, *124*, 14814-14815. (b) Miyoshi, Y.; Akatsuka, T.; Okuoka, S.; Tsukajima, A.; Makino, M.; Saito, M.; Yonehara, K. Palladium-Catalyzed Aerobic Intermolecular Cyclization of Acrylic Acid with 1-Octene to Afford α-Methylene-γ-butyrolactones: The Remarkable Effect of Continuous Water Removal from the Reaction Mixture and Analysis of Reaction by Kinetic, ESI-MS, and XAFS Measurements. *Chem. Eur. J*. **2012**, *18*, 7941-7949.

(21) Au: (a) Hashmi, A. S. K.; Lothschuetz, C.; Ackermann, M.; Doepp, R.; Anantharaman, S.; Marchetti, B.; Bertagnolli, H.; Rominger, F. Gold Catalysis: In Situ EXAFS Study of Homogenous Oxidative Esterification. *Chem. Eur. J*. **2010**, *16*, 8012-8019. (b) Nguyen, B. N.; Adrio, L. A. Barreiro, E. M.; Brazier, J. B.; Haycock, P.; Hii, K. K.; Nachtegaal, M.; Newton, M. A.; Szlachetko, J. Deconvolution of the Mechanism of Homogenous Gold-Catalyzed Reactions. *Organometallics* **2012**, *31*, 2395-2402.

(22) Cu: (a) He, C.; Zhang, G.; Ke, J.; Zhang, H.; Miller, J. T.; Kropf, A. J.; Lei, A. Labile Cu(I) Catalyst/Spectator Cu(II) Species in Copper-Catalyzed C-C Coupling Reaction: Operando IR, In Situ XANES/EXAFS Evidence and Kinetic Investigations. *J. Am. Chem. So*c. **2013**, *135*, 488-493. (b) Walroth, R. C.; Uebler, J. W. H.; Lancaster, K. M. Probing CuI in Homogenous Catalysis using High-Energy-Resolution Fluorescence-Detected X-Ray Absorption Spectroscopy. *Chem. Commun*. **2015**, *51*, 9864-9867.

(23) (a) Nelson, R. C.; Miller, J. T. An Introduction to X-Ray Absorption Spectroscropy and Its In Situ Application to Organometallic Compounds and Homogeneous Catalysts. *Catal. Sci. Tech*. **2012**, *2*, 461-470. (b) Stherborne, G. J.; Nguyen, B. N. Recent XAS Studies into Homogeneous Metal Catalyst in Fine Chemical and Pharmaceutical Syntheses. *Chem. Cent. J*. **2015**, *9*, 1-6. (c) Evans, T. Tilden Lecture: Shining Light on Metal Catalysts. *Chem. Soc. Rev*.**1997**, 11-19.

(24) (a) Wooley, M. J.; Khairallah, G. N.; Donnelly, P. S.; O' Hair, R. A. J. Nitrogen Adduction by Three Coordinate Group 10 Organometallic Cations: Platinum is Favored over Nickel and Palladium. *Rapid Commun. Mass Spectrom*. **2011**, *25*, 2083-2088. (b) Qian, B.; Guo, S.; Shao, J.; Zhu, Q.; Yang, L.; Xia, C.; Huang, H. Palladium-Catalyzed Benzylic Addition of 2-Methyl Azaarenes to N-Sulfonyl Aldimines via C-H Bond Activation. *J. Am. Chem. Soc*. **2010**, *132*, 3650-3651. (c) Hammer, C. F.; Heller, S. R.; Craig, J. H. Reactions of β-Substituted Amines. II. Nucleophilic Displacement Reactions on 3-Chloro-1-ethylpiperidine. *Tetrahedron* **1972**, *28*, 239-253.

(25) Markies, B. A.; Canty, A. J.; de Graaf, W.; Boersma, J.; Janssen, M. D.; Hogerheide, M. P.; Smeets, W. J.; Spek, A. L.; van Koten, G. Synthesis and Structural Studies of Phenyl(iodo)- and Methyl(phenyl)palladium(II) Complexes of Bidentate Nitrogen Donor Ligands. *J. Organomet. Chem*. **1994**, *482*, 191-199.

(26) Milani, B.; Alessio, E.; Mestroni, G.; Sommazzi, A.; Garbassi, F.; Zangrando, E.; Bresciani-Pahor, N.; Randaccio, L. Synthesis and Characterization of Monochelated Carboxylatopalladium(II) Complexes with Nitrogen-Donor Chelating Ligands. Crystal Structures of Diacetato(1,10-phenanthroline)- and Diacetato(2,9-dimethyl-1,10-phenanthroline)-palldium(II). *J. Chem. Soc., Dalton Trans*. **1994**, 1903-1911.

(27) A related rapid and reversible reductive elimination between the acetato and allyl at Pd(II) was reported: Yamamoto, T.; Akimoto, M.; Saito O.; Yamamoto, A. Interaction of Palladium(0) Complexes with Allylic Acetates, Allyl Ethers, Allyl Phenyl Chalcogenides, Allylic Alcohols, and Allylamines. Oxidative Addition, Condensation, Disproportionation, and π-Complex Formation. *Organometallics* **1986**, *5*, 1559-1567.

(28) (a) Obora, Y.; Tsuji, Y.; Nishiyama, K.; ebihara, M.; Kawamura, T. Structure and Fluxional Behavior of *cis*-Bis(stannyl)bis(phosphine)platinum: Oxidative Addition of Organodistannane to Platinum(0) Complex. *J. Am. Chem. Soc*. **1996**, *118*, 10922-10923. (b) Tsuji, Y.; Nishiyama, K.; Hori, S.; Ebihara, M.; Kawamura, T. Structure and Facile Unimolecular Twist-Rotation of *cis*-Bis(silyl)bis(phosphine)platinum and *cis*-Bis(stannyl))bis(phosphine)palladium Complexes. *Organometallics* **1998** *17*, 507-512. (c) Ozawa, F.; Kamite, J. Mechanistic Study on the Insertion of Phenylacetylene into *cis*-Bis(silyl)platinum(II) Complexes. *Organometallics* **1998**, *17*, 5630-5639.

(29) (a) Calligaris, M.; Carugo, O. Structure and Bonding in Metal Sulfoxide Complexes. *Coord. Chem. Rev*. **1996**, *153*, 83-154. (b) Diao, T.; White, P.; Guzei, I.; Stahl, S. S. Characterization of DMSO Coordination to Palladium(II) in Solution and Insights into the Aerobic Oxidation Catalyst, $Pd(DMSO)_2(TFA)_2$. *Inorg. Chem*. **2012**, *51*, 11898-11909.

(30) Kirchberg, S.; Tani, S.; Ueda, K.; Yamaguchi, J.; Studer, A.; Itami, K. Oxidative Biaryl Coupling of Thiophenes and Thiazoles with Arylboronic Acids through Palladium Catalysis: Otherwise Difficult C4-Selective C-H Arylation Enabled by Boronic Acids. *Angew. Chem. Int. Ed*. **2011**, *50*, 2387-2391.

(31) Ye, M.; Gao, G.-L.; Yu, J.-Q. Ligand-Promoted C-3 Selective C-H Olefination of Pyridines with Pd Catalysts. *J. Am. Chem. Soc*. **2011**, *133*, 6964-6967.

(32) (a) Halligudi, S. B.; Khan, N. H.; Kureshy, R. I.; Suresh, E.; Venkatsubramanian, K. Synthesis, Structural Characterization and Catalytic Carbonylation of Nitrobenzene to Phenylurethane using Palladium(II) 1,10-Phenanthroline Diacetato Complex. *J. Mol. Catal. A*, **1997**, *124*, 147-154. (b) Ragaini, F.; Gasperini, M.; Cenini, S.; Arnera, L.; Caselli, A.; Macchi, P.; Casati, N. Mechanistic Study of the Palladium-phenanthroline Catalyzed Carbonylation of Nitroarenes and Amines: Palladium-Carbonyl Intermediates and Bifunctional Effects. *Chem. Eur. J*. **2009**, *15*, 8064-8077.

(33) Devereux, M.; O' Shea, D.; O' Connor, M.; Grehan, H.; Connor, G.; McCann, M.; Rosair, G.; Lyng, F.; Kellett, A.; Walsh, M.; Egan, D.; Thati, B. Synthesis, Catalase, Superoxide Dismutase and Antitumor Activities of Copper(II) Carboxylate Complexes Incorporating Benzimidazole, 1,10-Phenanthroline and Bipyridine Ligands: X-ray Crystal Structures of $[Cu(BZA)_2(bpy)(H_2O)]$[, $[Cu(SalH)_2(BZDH)_2]$ and $[Cu(CH_3COO)_2(5,6\text{-}DMBZDH)_2]$. *Polyhedron* **2007**, *26*, 4073-4084.

(34) Barquín, M.; González Garmendia, M. J.; Larrínaga, L.; Pinilla, E.; Torres, M. R. Complexes of $Cu_2(\mu\text{-}OAc)_4(H_2O)_2$ with 1,10-Phenathroline and Comparison with Those of 2,2'-Bipyridne. Crystal Structure of the Dimer $[Cu(OAc)_2(phen)](\mu\text{-}H_2O)$. *Z. Anorg. Allg. Chem*. **2005**, *631*, 2151-2155.

(35) (a) Kresge, A.; Brennan, J. Perchloric Acid Catalyzed Aromatic Mercuration in Acetic Acid Solution. II. The Substitution Process. *J. Org. Chem*. **1967**, *32*, 752-755. (b) Fung, C. W.; Khorramdel-Vahed, M.; Ranson, R. J.; Roberts, R. M. G. Kinetics and Mechanism of Mercuation of Aromatic Compounds by Merury Trifluoroacetate in Trifluoroacetic Acid. *J. Chem. Soc. Perkin Trans 2* **1980**, 267-272.

(36) Yagyu, T.; Hamada, M.; Osakada, K.; Yamamoto, T. Cationic Arylpalladium Complexes with Chelating Diamine Ligands, $[PdAr(N\text{-}N)(solv)]BF_4$ (N-N = *N,N,N',N'*-tetramethylethylenediamine, 2,2'-bipyridine, 4,4'-dimethyl-2,2'-bipyridine). Preparation, Intermolecular Coupling of the Aryl Ligands, and Insertion of Alkyne and Allene into the Pd-C Bond. *Organometallics* **2001**, *20*, 1087-1101.

(37) Osakada, K.; Onodera, H.; Nishihara, Y. Diarylpalladium Complexes with a Cis Structure. Formation via Transmetalation of Arylboronic Acids with and Aryliodopalladium Complex and Intramolecular Coupling of the Aryl Ligands, Affording Unsymmetrical Biaryls. *Organometallics* **2005**, *24*, 190-192.

(38) (a) Mitsudome, T.; Yoshida, S.; Mizugaki, T.; Jitsukawa, K.; Kaneda, K. Highly Atom-Efficient Oxidation of Electron-Defi-

cient Internal Olefins to Ketones Using a Palladium Catalyst. *Angew. Chem. Int. Ed.* **2013**, *52*, 5961-5964. (b) Mitsudome, T.; Yoshida, S.; Tsubomoto, Y.; Mizugaki, T.; Jitsukawa, K.; Kaneda, K. Simple and Clean Synthesis of Ketones from Internal Olefins Using $PdCl_2$/*N,N*-Dimethylacetamide Catalyst System. *Tetrahedron Lett.* **2013**, *54*, 1596-1598. (c) Mitsudome, T.; Mizumoto, K.; Mizugaki, T.; Jitsukawa, K.; Kaneda, K. Wacker-Type Oxidation of Internal Olefins Using a $PdCl_2$/*N,N*-Dimethylacetamide Catalyst System under Copper-Free Reaction Conditions. *Angew. Chem. Int. Ed.* **2010**, *49*, 1238-1240. A concise review on Pd-catalyzed aerobic oxidation reactions is reported. *See* ref. 10d.

(39) The Pd K-edge (24.357 keV) XAFS data were collected by transmission mode under air and calibrated by using a Pd foil as a reference. For solution-phase XAFS of **1a** and **1b**, we used dimethyl phthalate as the solvent and measured the solution after filtration with a PTFE Milipore filter (pore size: 0.2 μm) by use of a cylindrical glass cell (10 mm i.d. x 100 mm) for JASCO polarimeter.

(40) Boron nitride (BN) is widely used to dilute a solid sample for XAS study because BN is almost transparent to the synchrotron radiation.

(41) Calvin, S. *XAFS for Everyone*; CRC: Boca Raton, 2013; pp.224-225.

(42) The fitting calculations were performed by FEFF6 program (revision 9.6.4) embedded with Artemis where the theoretical scattering paths were generated from the Cartesian coordinates based on the DFT calculations of **1b** and **1c** depicted in Figure 4. *FEFF9 program*: Rehr, J. J.; Kas, J. J.; Vila, F. D.; Prange, M. P.; Jorissen, K. Parameter-Free Calculations of X-ray Spectra with FEFF9. *Phys. Chem. Chem. Phys*. **2010**, *12*, 5503-5513. *Athena and Artemis program*: (a) Newville, M. IFEFFIT: Interactive XAFS Analysis and FEFF Fitting. *J. Synchrotron Rad.* **2001**, *8*, 322-324. (b) Ravel, B.; Newville, M. ATHENA, ARTEMIS, HEPHAESTUS: Data Analysis for X-Ray Absorption Spectroscopy using IFEFFIT. *J. Synchrotron Rad*. **2005**, *12*, 537-541.

(43) Hosokawa, T.; Uno, T.; Inui, S.; Murahashi, S.-I. Palladium(II)-Catalyzed Asymmetric Oxidative Cyclization of 2-Allylphenols in the Presence of Copper(II) Acetate and Molecular Oxygen. Study of the Catalysis of the Wacker-type Oxidation. *J. Am. Chem. Soc*. **1981**, *103*, 2318-2323.

(44) Hosokawa, T.; Nomura, T.; Murahashi, S.-I. Palladium-Copper-DMF Complexes Involved in the Oxidation of Alkenes. *J. Organomet. Chem.* **1998**, *551*, 387-389.

(45) (a) Takahashi, T. Ito, S. Sakai, Y. Ishii, Novel Palladium(0) Complex; Bis(dibenzylideneacetone)palladium(0). *J. Chem. Soc., D; Chem. Commun*. **1970**, 1065-1066. (b) Ukai, T.; Kawazura, H.; Ishii, Y.; Bonnett, J. J.; Ibers, J. A. Chemistry of Dibenzylideneacetone-Palladium(0) Complexes. I. Novel Tris(dibenzylideneacetone)dipalladium(solvent) Complexes and Their Reactions with Quinones. *J. Organomet. Chem*. **1974**, *65*, 253-266. Related papers are as follows: (c) Zalesskiy, S. S.; Ananikov, V. P. $Pd_2(dba)_3$ as Precursor of Soluble Metal Complexes and Nanoparticles: Determination of Palladium Active Species for Catalysis and Synthesis. *Organometallics* **2012**, *31*, 2302-2309. (d) Kapdi, A. R.; Whitwood, A. C.; Williamson, D. C.; Lynam, J. M.; Burns, M. J.; Williams, T. J.; Reay, A. J.; Holmes, J.; Fairlamb, I. J. S. The Elusive Structure of $Pd_2(dba)_3$. Examination by Isotopic Labeling, NMR Spectroscopy, and X-ray Diffraction Analysis: Synthesis and Characterization of $Pd_2(dba\text{-}Z)_3$ Complexes. *J. Am. Chem. Soc.* **2013**, *135*, 8388-8399.

(46) Schulze, B. M.; Shewmon, N. T.; Zhang, J.; Watkins, D. L.; Mudrick, J. P.; Cao, W.; Bou Zerdan, R.; Quaretarao, A. J.; Ghiviriga, I.; Xue, J.; Castellano, R. K. Consequences of Hydrogen Bonding on Molecular Organization and Charge Transport in Molecular Organic Photovoltaic Materials. *J. Mater. Chem. A* **2014**, *2*, 1541-1549.

(47) (a) Feng, M.-L.; Li, Y.-F.; Zhu, H.-J.; Zhao, L.; Xi, B.-B.; Ni, J.-P. Synthesis, Insecticidal Activity, and Structure-Activity Relationship of Trifluoromethyl-Containig Phthalic Acid Diamide Structures. *J. Agric. Food Chem*. **2010**, *58*, 10999-11006. (b) Ruchelman, A. L.; Muller, G. W.; Man, H.-W. JP5927241 B2, 2016.. (c) Hiraiwa, Y.; Ida, M.; Kudo, T.; Morinaka, A.; Chikauchi, K.; Mori, K. Patent WO 2008016007 A1, 2008. (d) van Antwerpen, P.; Prévost, M.; Zouaoui-Boudjeltia, K.; Babar, S.; Legssyer, I.; Moreau, P.; Moguilevsky, N.; Vanhaeverbeek, M.; Ducobu, J.; Nève, J.; Dufrasne, F. Conception of Myeloperoxidase Inhibitors Derived from Flufenamic Acid by Computational Docking and Structure Modification. *Bioorg. Med. Chem*. **2008**, *16*, 1702-1720.

(48) Roubinet, B.; Weber, M.; Shojaei, H.; Bates, M.; Bossi, M. L.; Belov, V. N.; Irie, M.; Hell, S. W. Fluorescent Photoswitchable Diarylethenes for Biolabeling and Single-Molecule Localization Microscopies with Optical Superresolution. *J. Am. Chem. Soc.* **2017**, 139, 6611-6620.

(49) *CrystalStructure* ver. 4.2; Rigaku Corporation, Tokyo, Japan, 2015.

(50) Sheldrick, G. *SHELXL97*; University of Göttingen, Germany, 1997.

(51) *POV-Ray for Windows*, ver. 3.6.2; Persistence of Vision Ray Tracer Pty, Ltd.

Table of Contents Graphic